HHS Public Access

Author manuscript

J Med Chem. Author manuscript; available in PMC 2021 November 16.

Published in final edited form as:

J Med Chem. 2021 April 08; 64(7): 4239–4256. doi:10.1021/acs.jmedchem.1c00268.

2,4,5-Trisubstituted Pyrimidines as Potent HIV-1 NNRTIs: Rational Design, Synthesis, Activity Evaluation, and Crystallographic Studies

Dongwei Kang[†,&,*], **Francesc X. Ruiz**[φ,ǀ], **Yanying Sun**[†], **Da Feng**[†], **Lanlan Jing**[†], **Zhao Wang**[†], **Tao Zhang**[†], **Shenghua Gao**[†], **Lin Sun**[†], **Erik De Clercq**[§], **Christophe Pannecouque**[§], **Eddy Arnold**[φ,ǀ,*], **Peng Zhan**[†,&,*], **Xinyong Liu**[†,&,*]

[†]Department of Medicinal Chemistry, Key Laboratory of Chemical Biology (Ministry of Education), School of Pharmaceutical Sciences, Cheeloo College of Medicine, Shandong University, 44 West Culture Road, 250012 Jinan, Shandong, PR China

[§]Rega Institute for Medical Research, Laboratory of Virology and Chemotherapy, K.U. Leuven, Herestraat 49 Postbus 1043 (09.A097), B-3000 Leuven, Belgium.

[φ]Center for Advanced Biotechnology and Medicine, Rutgers University, Piscataway, New Jersey, 08854, United States

[ǀ]Department of Chemistry and Chemical Biology, Rutgers University, Piscataway, New Jersey, 08854, United States

[&]China-Belgium Collaborative Research Center for Innovative Antiviral Drugs of Shandong Province, 44 West Culture Road, 250012 Jinan, Shandong, PR China

Abstract

There is an urgent unmet medical need for novel HIV-1 inhibitors that are effective against a variety of NNRTI-resistance mutations. We report our research efforts aimed at discovering a novel chemotype of anti-HIV-1 agents with improved potency against a variety of NNRTI-resistance mutations in this paper. Structural modifications of the lead **K-5a2** led to the identification of a potent inhibitor **16c**. **16c** yielded highly potent anti-HIV-1 activities and improved resistance profiles compared with the approved drug etravirine (ETR). The co-crystal structure revealed the key role of the water networks surrounding the NNIBP for binding and for resilience against resistance mutations, while suggesting further extension of **16c** towards the NNRTI-adjacent site as lead development strategy. Furthermore, **16c** demonstrated favorable pharmacokinetic and safety properties, suggesting the potential of **16c** as a promising anti-HIV-1 drug candidate.

[*]**Corresponding Authors**: D.K.: kangdongwei@sdu.edu.cn; tel, 086-531-88382005; E. A.: arnold@cabm.rutgers.edu; tel, 848-445-9777; P.Z.: zhanpeng1982@sdu.edu.cn; tel, 086-531-88382005; X.L.: xinyongl@sdu.edu.cn; tel, 086-531-88380270.

Supporting Information includes:

In vitro assay of anti-HIV activities in MT-4 cells, recombinant HIV-1 reverse transcriptase (RT) inhibitory assays, pharmacokinetic methods, acute toxicity experiment, and assay procedures for hERG activity (PDF).

The authors declare that all experimental work complied with the institutional guidelines on animal studies (care and use of laboratory animals).

The authors declare no competing financial interest.

INTRODUCTION

Acquired immunodeficiency syndrome (AIDS) is caused by human immunodeficiency virus type 1 (HIV-1), becoming a pandemic health problem which globally affects nearly 38.0 million people and with 1.7 million newly infected with HIV in 2019.[1] In the HIV-1 infection process, HIV-1 reverse transcriptase (RT) is responsible for the reverse transcription of single-stranded RNA into double-stranded DNA.[2] With RT as target, eight nucleoside/nucleotide RT inhibitors (NRTIs/NtRTIs) and six non-nucleoside RT inhibitors (NNRTIs) have been approved by the U.S. Food and Drug Administration (FDA) so far.[3,4] NRTIs are analogues of the natural substrate deoxynucleotide triphosphates and they inhibit RT as chain terminators, while NNRTIs do not compete for the natural substrate, they bind in the NNRTI binding pocket (NNIBP) about 10 Å away from the polymerase active site known and acted as allosteric inhibitors.[5] Therein, NNRTIs are widely used in combination antiretroviral therapy (cART) with the advantage of their promising antiviral activity and higher selectivity. Currently FDA-approved NNRTIs in clinical use include the first-generation NNRTIs nevirapine (NVP), delavirdine (DLV), efavirenz (EFV), and the second generation NNRTIs etravirine (ETR), rilpivirine (RPV) and doravirine (DOR).[3, 4] However, NNIBP residues are not involved in the polymerase binding site, and their mutations do not have significant effect on replication. Thus, the NNRTIs have a low genetic barrier and NNRTI resistance mutations appear relatively easy and fast.[5] The first-generation NNRTIs quickly suffered from drug resistance, including single mutations (K103N and Y181C) and double mutation K103N+Y181C (RES056). Although the second generation exhibited these mutations sensitive to the first-generation NNRTIs, drug resistance and cross resistance still emerged with their clinical use. In addition, the adverse effects (such as hypersensitivity reactions) can also result in treatment failure of the second generation NNRTIs.[6, 7] Therefore, there is a relevant need of novel NNRTIs with greater potency, improved drug-resistance profiles and safety.

Our previous efforts have prompted the discovery of novel piperidine-substituted thiophene[3,2-*d*]pyrimidine compounds **3** (**K-5a2)** and **4** (**25a**), exhibiting higher anti-HIV-1 potency and favorable resistance profiles compared with ETR and RPV.[8, 9] The co-crystal structures revealed extensive hydrophobic interactions and a network of backbone hydrogen bonds formed between the NNRTIs and NNIBP, and explained why **K-5a2** and **25a** are resilient to NNRTI-resistance mutations in the NNIBP.[10] Although **K-5a2** and **25a** developed extensive interactions with NNIBP and their central thiophene[3,2-*d*]pyrimidine core establishes nonpolar interactions with the alkyl chain of Glu138, the entrance channel gated by Glu138 in the p51 subunit and Lys101 in the p66 subunit is still an underexplored region in the NNIBP.

In this study, we have kept the privileged left wing and piperidine-substituted benzyl of **K-5a2** unchanged,[8, 11] and 18 novel 2,4,5-trisubstituted pyrimidine derivatives (**11-16**) with 2-thienyl, 3-thienyl, 2-furyl, 3-furyl, phenyl and 4-pyridyl linked to the C_5 position of the central pyrimidines were designed utilizing a scaffold hopping strategy, to get a deeper insight of the structure-activity relationships (SARs) of the NNIBP Tolerant Region II (Figure 2).[12] The preliminary results demonstrated that the disruption of the molecular

planarity of the fused bicyclic thiophene[3,2-*d*]pyrimidine was a valuable strategy for the subsequent optimization of our lead compounds and the introduction of a pyridine ring in the Tolerant Region II is the most beneficial modification for the activity. Moreover, multiple substituent groups were introduced into the pyridine ring in the second-round structural modification, and yielded 27 novel derivatives. In addition, the privileged cyanovinyl group was merged into the left wing of the compounds,[9, 13-15] to develop stronger **π-π** interactions with conserved amino acids F227 and W229 (Figure 2).

CHEMISTRY

As depicted in Schemes 1 and 2, two short synthetic protocols that would allow the rapid optimization of the two variable points (R^1 and Ar) were used to produce the newly designed compounds. At first, the commercially available material 2,4-dichloropyrimidine (**5**) was reacted with 4-hydroxy-3,5-dimethylbenzonitrile at room temperature, affording intermediate **6**, which generated compound **7** with *tert*-butyl 4-aminopiperidine-1-carboxylate at 120°C *via* nucleophilic reaction. Compound **7** was treated with NIS and HOAc to form compound **8**; subsequent treatment of which in the presence of trifluoroacetic acid afforded product **9**. Then treatment of **9** with substituted benzyl chloride (bromine) at room temperature yielded the key intermediates **10a-c**, which were finally coupled with boric acid substituents in the presence of potassium carbonate and $Pd(PPh_3)_4$ at 100°C *via* Suzuki reaction, to afford the corresponding target compounds **11-16**. In an analogous way, target compounds **22-30** were prepared, only with the difference that the starting material **5** was treated with (*E*)-3-(4-hydroxy-3,5-dimethylphenyl)acrylonitrile.

BIOLOGY

HIV-1 RT Crystallization and Structure Determination

An engineered HIV-1 RT construct, RT52A, referred to as wild-type (WT) RT, was expressed and purified as described previously.[16, 17] RT52A (20 mg mL^{-1}) was incubated with **16c** at a 1:1.5 protein:drug molar ratio at room temperature for 30 min. Co-crystals of RT with **16c** were set up in hanging drops at 4°C with a 1:1 ratio of protein-ligand complex and reservoir (10%(*v*/*v*) PEG 8000, 4%(*v*/*v*) PEG 400, 100 mM MES pH 6.3, 10 mM spermine, 15 mM $MgSO_4$, 100 mM ammonium sulfate, and 5 mM tris(2-carboxyethyl)phosphine) together with an experimentally optimized concentration of microseeds made by crushing previously obtained RT/rilpivirine crystals (pre-seeding). The crystals were cryo-protected by dipping them into reservoir with 25% ethylene glycol and plunge-frozen in liquid N_2. X-ray data were collected from three of the plunge-frozen crystals at the APS 23-ID-B beamline. The crystallographic software packages HKL2000,[18] Phenix,[19] and COOT[20] were used for data processing, structure refinement, and model building, respectively. **16c** coordinates and restraints were generated with the Grade Web Server (http://grade.globalphasing.org). The structure was solved by molecular replacement using PDB ID 4G1Q as the template. The diffraction data and refinement statistics are summarized in Table S1.

RESULTS AND DISCUSSION

First Round of Structural Modification

All of the synthesized inhibitors possessing the 2,4,5-trisubstituted pyrimidine scaffold of the first round (**11-16**) were firstly screened for their biological activity *in vitro* against wild-type (WT) HIV-1 (IIIB), as well as against the NNRTI-resistant strain K103N+Y181C (RES056) using the MTT method according to previously reported procedures,[21, 22] with the aim of getting the first insight into the SAR and to identify the most promising candidates for further optimization. The second-generation NNRTI drugs ETR and RPV were selected as controls. The values of EC_{50} (anti-HIV potency), CC_{50} (cytotoxicity), and SI (selectivity index, CC_{50}/EC_{50} ratio) of the synthesized compounds were determined.

As shown in Table 1, **14a** (EC_{50} = 2.80 nM) was demonstrated to be the most promising inhibitor against HIV-1 IIIB, being comparable to that of the approved drug ETR (EC_{50} = 2.80 nM). Moreover, all synthesized inhibitors exhibited high effective activity against the HIV-1 IIIB strain with EC_{50} values ranging from 2.51 to 5.93 nM. The substitution pattern of Ar and R^1 did not significantly influence the compounds' antiviral profile against HIV-1 IIIB. However, the Ar group located in the Tolerant Region II could result in significant differences in activity to mutant HIV-1 strain RES056. On the whole, most of the compounds experienced a dramatic activity drop to a micromolar level of inhibition against RES056. **15a-c** (Ar = phenyl) exhibited the weakest potency, with EC_{50} values of 427-590 nM, being much inferior to that of ETR (EC_{50} = 37.6 nM) and RPV (EC_{50} = 10.7 nM). Changing the phenyl substituent of **15a-c** to thienyl (**11a-c** and **12a-c**) and furyl (**13a-c** and **14a-c**) improved the compounds' activity (EC_{50} = 115-415 nM). More specifically, **11a-c** (EC_{50} = 103-134 nM) with 2-thienyl substituent exhibited more potent activity than those of **12a-c** (EC_{50} = 209-415 nM) with 3-thienyl substituent, while **13a-c** (EC_{50} = 218-254 nM) with 2-furyl substituent exhibited decreased activity compared to those of **14a-c** (EC_{50} = 108-172 nM) with the 3-furyl substituent. Replacement of phenyl substituent of **15a-c** with 4-pyridyl substituent also increased the compounds' potency (**16a-c**, EC_{50} = 24.4-244 nM), especially, **16c** (EC_{50} = 24.4 nM) yielded the greatest potency against mutant strain RES056, being superior to that of ETR (EC_{50} = 37.6 nM) and slightly inferior to RPV (EC_{50} = 10.7 nM). Notably, **16c** displayed much lower cytotoxicity (CC_{50} = 36.0 μM) and higher SI values against HIV-1 IIIB and RES056 strain (SI = 9603 and 1474, respectively) compared to that of RPV (CC_{50} = 3.98 μM, SI = 3989 and 371, respectively). None of the tested compounds showed anti-HIV-2 ROD activity.

Moreover, all these compounds were further evaluated for their activity against single mutant strains L100I, K103N, Y181C, Y188L, and E138K, and double-mutant strain F227L + V106A. As displayed in Table 2, the most promising mutant HIV-1 strain RES056 inhibitor **16c** also exhibited effective potency against all tested mutant strains, with EC_{50} values of 4.26 nM (L100I), 3.79 nM (K103N), 6.79 nM (Y181C), 6.79 nM (Y188L), 10.9 nM (E138K), and 10.4 nM (F227L+V106A), being equipotent to or superior to ETR and RPV in the same cellular assay. Specifically, in the case of Y188L and F227L+V106A mutant strains, **16c** showed 11-fold and 7.8-fold activity enhancement over that of RPV (EC_{50} = 79.4 nM and 81.6 nM), respectively.

In addition, most compounds were potent inhibitors against K103N, Y181C, Y188L, and E138K strains, with EC_{50} values ranging from 2.33 nM to 35.5 nM. However, apart from **16c**, all the compounds exhibited inferior potency (EC_{50} = 5.92-151 nM and 30.2-393 nM, respectively) compared to that of ETR (EC_{50} = 5.42 nM and 17.5 nM, respectively) against the L100I and F227L+V106A strains. The first round of SAR results indicated that, among all the employed substituents in the first round of this study, the 4-pyridyl group was the best choice for the NNIBP Tolerant Region II.

Second Round of Structural Modification

Based on the preliminarily established SARs, 27 novel 2,4,5-trisubstituted pyrimidine derivatives (**22-30**) were designed with the most promising inhibitor **16c** as lead. These newly designed compounds retained the privileged piperidine-substituted benzyl as their right wing; the cyano group in the left wing was replaced with a cyanovinyl group, to develop stronger π-π interactions with the highly conserved residues F227 and W229;[9] meanwhile, fluorine, chlorine, bromine, methyl, methoxy, and amino substituents were also introduced into the 4-pyridyl moiety located in Tolerant Region II, to explore the SARs of Tolerant Region II more comprehensively. All derivatives **22-30** from the second round were assayed *in vitro* for their activity against HIV-1 IIIB and RES056. The results of this evaluation are summarized in Table 3.

The compounds generated in the second round contain the privileged 2,4,5-trisubstituted pyrimidine scaffold, and displayed nanomolar activity against HIV-1 IIIB with EC_{50} values of 3.95-8.26 nM, being comparable to that of ETR (EC_{50} = 3.53 nM). More encouragingly, their activity against the mutant HIV-1 strain RES056 was significantly increased, yielding EC_{50} values ranging from 20.4 nM to 40.3 nM, and being about 2-fold more potent than that of ETR (EC_{50} = 52.2 nM), with the exception of compounds **25c** (EC_{50} = 53.4 nM) and **26c** (EC_{50} = 81.7 nM). However, the introduction of a cyanovinyl group substituent resulted in these compounds having enhanced cytotoxicity (CC_{50} = 2.10-25.3 μM) compared to the lead **16c** (CC_{50} = 36.0 μM). Although the cyanovinyl group was favorable for improving potency against mutant strains, it could result in potential covalent binding with nucleic acids or proteins as a “Michael acceptor” and cause an increase of cytotoxicity.[21] When comparing the cytotoxicity of these target compounds, **28a-c** tolerating the 3-pyridyl in the Tolerant Region II showed the lowest cytotoxicity, exhibiting CC_{50} values of 20.4-25.3 μM. However, harboring an amino group or fluorine atom on the 3-pyridyl substituent resulted in compounds **29a-c** (CC_{50} = 2.39-12.8 μM) and **30a-c** (CC_{50} = 6.05-20.9 μM), respectively, which resulted in increased cytotoxicity. Replacing the 3-pyridyl of **28a-c** with 4-pyridyl resulted in compounds **22a-c** (CC_{50} = 7.20-10.2 μM), which exhibited enhanced cytotoxicity. Also, the introduction of fluorine, chlorine, bromine, methyl, methoxy, or amino substituent on the 4-pyridyl moiety of **22a-c** led to greater cytotoxicity.

Furthermore, eight compounds (**22a**, **22c**, **28a-c**, **29c**, **30a**, and **30c**) that exhibited higher potency and lower cytotoxicity were further evaluated for their activity against HIV-1 viral isolates carrying a variety of NNRTI-resistance mutations. As depicted in Table 4, although most of the selected compounds demonstrated more potent activity against L100I, Y181C, E138K and F227L+V106A strains than did ETR, all of the compounds exhibited inferior

potency (EC_{50} = 3.84-7.50 nM, and 22.7-54.2 nM, respectively) compared to ETR (EC_{50} = 3.77 and 1.31 nM, respectively) and RPV (EC_{50} = 18.8 and 5.75 nM, respectively) for the most common mutant strains K103N and Y188L. The anti-HIV-1 results of two rounds of structural modification led to the conclusion that compound **16c** was the most potent among all the novel synthesized compounds, exhibiting higher potency against a panel of NNRTI-resistant strains than that of ETR and deserving further druggability evaluation.

Inhibition of WT HIV-1 RT by the Representative Compounds.

Some representative compounds (**14a**, **16c**, **22a**, and **22c**) were assayed *in vitro* for their ability to inhibit recombinant WT HIV-1 RT enzyme, and the results are summarized in Table 5. **14a**, **16c**, **22a**, and **22c** (IC_{50} = 0.092, 0.113, 0.143, and 0.102 μM, respectively) exhibited modest inhibitory activity against WT HIV-1 RT with IC_{50} values of 0.092, 0.113, 0.143, and 0.102 μM, being about 3.5-5.5-fold potent than that of NVP (IC_{50} = 0.510 μM). Although these novel inhibitors exhibited inferior activity compared to that of ETR (IC_{50} = 0.012 μM), the preliminary results validate their binding target is HIV-1 RT, and they are classical NNRTIs.

Crystal Structure of HIV-1 RT in Complex with 16c: Implications for Further Lead Development

To observe the detailed interactions between **16c** and the NNIBP (formed by three channels named tunnel, entrance and groove), the co-crystal structure of WT RT in complex with **16c** was determined at 2.02 Å resolution (Table S1 and Figure S1). As expected, the structure waas almost identical to that of the related RT complexes with **K-5a2** and **25a** (Figure S1F). Figure 3A depicts the main interactions of **16c** with RT. The left wing of **16c** is snuggling into the tunnel *via* hydrophobic interactions with Y181 and Y188 at one side, and P95 and L234 at the other. Meanwhile, the right wing is anchored into the groove by a hydrogen bond with the main-chain carbonyl of K101 and through hydrophobic contacts with L100, Y318, and P236. The central pyrimidine moiety is located in the entrance, surrounded by E138 of p51, L100 (hydrophobic contacts), and K101 (hydrogen-bonded to the main-chain amino group through a water bridge).

The 4-pyridyl substituent, as envisioned, sits in the solvent-exposed area in the vicinity of the entrance channel, displacing three water molecules (modeled in the RT-**16c** structure as an alternate conformation) observed in the RT-RPV high resolution structure (Figures 3B, **S1B** and **S1E**).[23] Moreover, it forms hydrophobic interactions with the side chains of V179 and Y181, and it is water-bridged to the main-chain carbonyl of I180 (Figure 3B). Notably, in all three RT structures with **K-5a2**, **25a**, and RPV, their central ring forms a water-mediated hydrogen bonding network with the main-chain atoms of E138 and of I180.[10, 23] Herein, the water molecule hydrogen-bonded to the central ring and E138 is displaced (alt-HOH 1 in Figure 3B), but the second water molecule hydrogen-bonded to I180 is conserved.

The RT-**16c** structure illustrates the importance of ordered water networks in NNRTI binding (Figures 3C-E). The left wing of **16c** makes a hydrogen bond with an interfacial water that is in turn hydrogen-bonded to the side chain of Y188 and the main chain of L228 (Figure

3C). Next, as mentioned, the entrance channel displays another interfacial water, which is connected to a succession of water molecules that end up in a water molecule bridging Q161, T165, and Q182, the latter being hydrogen-bonded to the main chain of M184 (Figure 3D), a residue that is part of the catalytic motif YMDD.[24] Both the left wing interfacial water and the ordered network near the entrance channel are observed in the RT-RPV high resolution structure (data not shown).[23] Lastly, the right wing of **16c** is also interacting with a water network bridging it to RT (Figure 3E). Central to it, HOH 2 connects the pyrimidine ring with the main chain of K101. At one end, the water network ends with HOH 1, hydrogen-bonded to p51's E138 side chain. At the other end, the water network finishes with HOH 4, which would be in the right position to be bonded to alt-HOH 3, expelled by the binding. The last is hydrogen bonded to the other carboxylic oxygen of p51's E138 side chain. This network is observed, albeit with some discontinuity, in the case of parent lead **K-5a2**. Interestingly, in the RT-RPV structure, there is a direct hydrogen bond between the main chain of K101 and the central ring, while the terminal amino group of the side chain of K101 overlaps with HOH 1 of RT-**16c** (present also in RT- **K-5a2**). Thus, in a different manner, all three complexes maintain a similar architecture in that part in between the entrance and the groove channels.

The RT-**16c** structure suggests that, not only the hydrogen bonds in the right wing and the several hydrophobic contacts all around the ligand, but also the water molecules (and networks) may anchor the compound in the NNIBP. While in the current structure the right-wing top amide group is not hydrogen-bonded (or with a polar interaction) with RT or has water molecules in the vicinity, both RPV (*i.e.*, nitrile substituent of the right wing with the carbonyl group of H235) and **K-5a2** (*i.e.*, hydrogen bonds to K104 and V106) present one or the other. In the case of RT-RPV, molecular dynamics (MD) simulations suggest as well the existence of a water molecule hydrogen-bonded to the benzonitrile in the right wing, as this area is solvent exposed.[10, 23]

Regarding the SAR, the structure points to all the different compounds binding roughly identically in terms of both the two wings and the central core, as well as for the different Ar substituents. Indeed, this is supported by the very similar antiviral activity of all of the tested compounds against strain IIIB (Tables 1-4) and in the *in vitro* activity assay (Table 5). The Ar substituents may thus displace the alternative conformation water molecules and will be engaged in hydrophobic contacts with the side chains of V179 and Y181 (Figure 3B). Meanwhile, the water-bridged interaction with I180 is potentially possible in all the compounds bearing an electronegative atom in the ring, able to function as a hydrogen bond acceptor. However, the geometry and/or distance may not be ideal in the five-membered rings. This interaction may be critical in the case of mutant strain RES056, where just compound **16c** can retain a similar antiviral activity as in the WT IIIB strain.

Structures of the K103N/Y181C mutant RT with RPV and compound **3** (**25a**) show that either the repositioning of the aromatic side chain of Y183 and/or maintaining the hydrogen-bonding interactions in the right wing may provide these adaptable compounds a similar tight interaction with WT RT.[10] Nevertheless, these interactions are expected to occur as well for both **16c** and the rest of compounds. Therefore, the interfacial water-mediated contact with I180 (connected to an extensive water network) may be the difference. This

contact is not possible in compounds **15a-c**, and likely suboptimal or not existing for compounds of the **11-14** series. What happens then with compounds **16a** and **16b**? The response is not apparent from this series, but from the second round of compounds designed after **16c** (Table 3). Compounds **22-30**, also resilient to K103N/Y181C mutations as **16c**, differ from compounds of the **16** series in that the ring wing bears the cyanovinyl group substituent instead of the cyano.

Notably, our previous high-resolution RT/RPV structure, combined with infrared spectroscopy experiments and MD simulations of WT and K103N/Y181C mutant RT,[23] shows that the conserved interaction of the cyanovinyl group with a water molecule contributes to the enhanced binding of RPV in both the WT and the mutant. This water molecule is conserved in the RT-**16c** structure, the first time this is observed with a left wing benzonitrile substituent. Thus, while the geometry is similar, the hydrogen bond is weaker in the current structure (2.7 Å in RT-RPV *vs.* 3.7 Å in RT-**16c**). We surmise that **16c**, but not **16a** or **16b**, is the only compound of the first round series presenting this water molecule (which in the RT-RPV structure is seen connected to a water network extending towards residues 224-226). Accordingly, compounds **22-30,** with the longer cyanovinyl group likely forming this water interaction, cope similarly well with the K103N/Y181C mutations irrespective of the R_1 substituent.

Overall, the analysis of the RT-**16c** structure and related SAR put the spotlight on the key role of the water networks around the NNIBP for tight ligand binding to both WT and mutant RT. In relation to it, several recent papers, by combining MD simulations, high resolution X-ray and neutron crystallography, and isothermal titration calorimetry (ITC), have shown the paramount role of this kind of water networks in ligand binding, suggesting that “solvent structure is an evolutionary constraint on protein sequence that contributes to ligand affinity and selectivity.”[25-27]

We also have recognized that the 4-pyridyl substituent extends out of the NNIBP in the direction of fragment 1QP (Figures 3F-G) sitting on the NNRTI-adjacent site,[16] which may allow fragment linking/merging approaches. To note that fragment 1QP displaces most of the water molecules forming the water network shown in Figure 3D. Taking into account that the 4-pyridyl substituent displaces the water molecules near the entrance channel, a compound targeting both pockets, as designed and tested by us recently, will displace all the water molecules out of these pockets and likely accounting for an entropic gain.[28] Therefore, the further development of these kind of compounds is warranted. The second round of optimization also encourages us to further pursue this direction, as the substitutions assayed were probably oriented towards the solvent area (because of the likely penalty of facing the protein side, *i.e.*, near residue I180 main chain), not resulting in any improvement in comparison to **16c**.

In Vivo Pharmacokinetics Study

The *in vivo* pharmacokinetic profile of **16c** was evaluated in Sprague Dawley rats (Table 6 and Figure 4A). After a single 2 mg/kg *iv* dose, compound **16c** was characterized by a modest clearance (CL = 110 mL/min/kg) and half-life ($T_{1/2}$ = 2.46 h), the maximum

concentration (C_{max}) could be up to 278 ng/mL. Absorption of **16c** was evaluated after being dosed at 20 mg/kg, it reached maximum concentration (T_{max}) at 1.00 h with a C_{max} of 174 ng/mL and the half-life was 1.74 h. However, the oral bioavailability (*F*) was 15.3%, which need further improvement for a drug candidate.

Safety Assessment

Assessment of Acute Toxicity—Next, the acute toxicity test of **16c** was carried out. A total of 20 Kunming mice were randomly divided into two groups and given single oral doses of 0 mg/kg (control group) and 2000 mg/kg of **16c** on the first day, respectively. The mice did not exhibit any toxic symptoms or mortality immediately during the subsequent two weeks. Additionally, there was no abnormality of body weight changed (Figure 4B). The results demonstrated that **16c** was well-tolerated up to a dose of 2000 mg/kg with no acute toxicity.

Assessment of hERG activity—With the aim to estimate the potential risk for cardiotoxicity, **16c** was evaluated for its activity against the hERG potassium channel using manual patch-clamp electrophysiology approach, and terfenadine was selected as reference drug. As shown in Figure 5, **16c** exhibited an IC_{50} value of 1.19 μM, and demonstrated much reduced QT liability and lower hERG inhibition in comparison with that of the lead **K-5a2** (IC_{50} = 0.130 μM) and the approved NNRTIs drug RPV (IC_{50} = 0.50 μM)[29].

Conclusion

We have reported herein efforts to discover novel potent HIV-1 inhibitors by exploiting the underexplored Tolerant Region II of the NNIBP, and forty-five novel 2,4,5-trisubstituted pyrimidine derivatives were designed using a scaffold hopping approach. Notably, we could demonstrate that compound **16c**, designed by introducing a 4-pyridyl group in the C_5 position of the central pyrimidine scaffold, led to improved anti-HIV-1 potency against WT and mutant HIV-1 strains compared to that of ETR, with EC_{50} values of 3.75 nM (WT), 4.26 nM (L100I), 3.79 nM (K103N), 6.79 nM (Y181C), 6.79 nM (Y188L), 10.9 nM (E138K), 10.4 nM (F227L+V106A), and 24.4 nM (RES056) in MT-4 cells. Moreover, **16c** exhibited lower cytotoxicity (CC_{50} = 36.0 μM), which contribute to its higher SI values toward WT and mutant HIV-1 strains. Additionally, **16c** exhibited *in vivo* favorable pharmacokinetic properties in Sprague Dawley rats (*F* = 15.3%) and safety in Kunming mice (LD_{50} > 2000 mg/kg).

The co-crystal structure and the SAR analysis, on the basis of the previous crystallographic and spectroscopic experiments and MD simulations, revealed that the water networks surrounding the NNIBP, both on top and on the bottom, may work as a sort of molecular staples anchoring the NNRTIs and allowing them to “wiggle and jiggle” (*i.e.*, conformational and positional adaptability) when resistance mutations arise. Furthermore, they provide a framework for an improved structure-based drug design of NNRTIs, especially those targeting simultaneously the NNIBP and the NNRTI Adjacent site.

EXPERIMENTAL SECTION

Chemistry

All melting points were determined on a micro melting point apparatus and are uncorrected. ^{1}H-NMR and ^{13}C-NMR spectra were recorded in $CDCl_3$ or DMSO-d_6 on a Bruker AV-400 spectrometer with tetramethylsilane (TMS) as the internal standard. A G1313A Standard LC Autosampler (Agilent) was used to collect samples for measurement of mass spectra. All reactions were monitored by thin layer chromatography (TLC), and spots were visualized with iodine vapor or by irradiation with UV light. Flash column chromatography was performed on columns packed with Silica Gel (200-300 mesh). Solvents were of reagent grade and were purified by standard methods when necessary. Compounds purity was analyzed on a Shimadzu SPD-20A/20AV HPLC system with a Inertsil ODS-SP, 5 μm C18 column (150 mm × 4.6 mm). HPLC conditions: methanol/ water 80:20; flow rate 1.0 mL/ min; UV detection from 210 to 400 nm; temperature, ambient; injection volume, 20 μL. Purity of all final compounds was >95%.

4-((2-chloropyrimidin-4-yl)oxy)-3,5-dimethylbenzonitrile (6)

To a solution of 4-hydroxy-3,5-dimethylbenzonitrile (1.47 g, 10 mmol) and K_2CO_3 (1.70 g, 12 mmol) in DMF (30 mL) was added 2,4-dichloropyrimidine (1.50 g, 10 mmol), and the resultant mixture stirred at room temperature for 5 h. The precipitated white solid was collected by filtration, washed with ice-water (100 mL), and recrystallized in DMF-H_2O to provide the intermediate **6** as a white solid in 90 % yield. ^{1}H NMR (400 MHz, DMSO-d_6) δ 8.70 (d, J = 5.7 Hz, 1H), 7.75 (s, 2H), 7.32 (d, J = 5.7 Hz, 1H), 2.10 (s, 6H). ESI-MS: m/z 260.3 $[M + H]^+$. $C_{13}H_{10}ClN_3O$ (259.05).

tert-butyl4-((4-(4-cyano-2,6-dimethylphenoxy)pyrimidin-2-yl)amino)piperidine-1-carboxylate (7)

A solution of **6** (0.26 g, 1.0 mmol), *N*-Boc-4-aminopiperidine (0.24 g, 1.2 mmol), and anhydrous K_2CO_3 (0.28 g, 2 mmol) in DMF (5 mL) was heated at 120°C for 12 h under magnetic stirring. Then the mixture wad cooled to room temperature and ice-water (40 mL) was added. The resulting precipitate was collected by filtration, and dried to give crude product, which was recrystallized from ethyl acetate (EA)/petroleum ether (PE) to afford the target compound **7** as a white solid in 69 % yield. ^{1}H NMR (400 MHz, DMSO-d_6) δ 8.20 (d, J = 5.5 Hz, 1H), 7.68 (s, 2H), 6.39 – 6.01 (m, 1H), 3.85 (s, 3H), 2.81 (dd, J = 63.9, 1.4 Hz, 3H), 2.08 (s, 6H), 1.64 (d, J = 80.2 Hz, 2H), 1.38 (d, J = 1.5 Hz, 9H), 1.23 (s, 2H). ESI-MS: m/z 424.5 $[M + H]^+$, 446.06 $[M + Na]^+$. $C_{23}H_{29}N_5O_3$ (423.23). HPLC purity: 99.28%.

tert-butyl4-((4-(4-cyano-2,6-dimethylphenoxy)-5-iodopyrimidin-2-yl)amino) piperidine-1-carboxylate (8)

Intermediate **7** (0.42g, 1.0 mmol) was added to a suspension of HOAc (0.30 g, 5.0 mmol) and NIS (0.34 g, 1.5 mmol) in acetonitrile (20 mL). The mixture solution was stirred for 4 h at room temperature; then, 10% Na_2CO_3 (1.06 g, 10.0 mmol) was added and the mixture was stirred for another 20 min. The obtained sloid was filtered and dried to give crude

product, which was recrystallized in EA to afford the target compound **8** as a white solid in 85 % yield. ESI-MS: m/z 550.4 $[M + H]^+$. $C_{23}H_{28}IN_5O_3$ (549.12). HPLC purity: 97.26%.

4-((5-iodo-2-(piperidin-4-ylamino)pyrimidin-4-yl)oxy)-3,5-dimethylbenzonitrile (9)

To a solution of **8** (0.55 g, 1.0 mmol) in dichloromethane (DCM) (4 mL) was added trifluoroacetic acid (TFA) (0.74 mL, 10 mmol) at room temperature, and the mixture was stirred for 6 h (monitored by TLC). Then, the reaction solution was alkalized to pH 9 with saturated sodium bicarbonate solution and extracted with DCM. The organic layer was washed with brine, dried over anhydrous Na_2SO_4, filtered and concentrated under reduced pressure to give **9** as a white solid in 89% yield. ^{1}H NMR (400 MHz, DMSO-d_6) δ 8.73 (s, 1H), 8.46 (s, 1H, C_6-pyrimidine-H), 7.70 (s, 2H), 7.37 (s, 1H), 3.03 – 2.97 (m, 2H), 2.09 (d, 6H), 1.97 – 1.37 (m, 7H). ESI-MS: m/z 450.3 $[M + H]^+$. $C_{18}H_{20}IN_5O$ (449.07). HPLC purity: 96.65%.

General procedure for the preparation of intermediates 10a-c

To a solution of **9** (0.45 g, 1.0 mmol) in anhydrous DMF (10 mL) was added anhydrous K_2CO_3 (0.28 g, 2.0 mmol) and substituted benzyl chloride (bromine) (1.2 mmol), and the solution was stirred for 4-7 h (monitored by TLC) at room temperature. The solvent was removed under reduced pressure and 30 mL water was added to the residue. Then the mixture solution was extracted with ethyl acetate and washed with saturated sodium chloride, purified by flash column chromatography and recrystallized from ethyl acetate (EA)/petroleum ether (PE) to afford the target compounds **10a-c**.

4-((4-((4-(4-cyano-2,6-dimethylphenoxy)-5-iodopyrimidin-2-yl)amino)piperidin-1-yl)methyl)benzenesulfonamide (10a)

White solid, 76 % yield, mp 145–147°C. ^{1}H NMR (400 MHz, DMSO-d_6) δ 8.42 (s, 1H, C_6-pyrimidine-H), 7.77 (d, J = 8.2 Hz, 2H), 7.69 (s, 2H), 7.45 (d, J = 8.1 Hz, 2H), 7.30 (s, 2H), 7.16 (s, 1H), 3.46 – 3.42 (m, 2H), 2.68 (s, 2H), 2.07 (s, 6H), 1.92 – 1.17 (m, 7H). ESI-MS: m/z 619.5 $[M + H]^+$. $C_{25}H_{27}IN_6O_3S$ (618.09). HPLC purity: 97.52%.

4-((5-iodo-2-((1-(4-(methylsulfonyl)benzyl)piperidin-4-yl)amino)pyrimidin-4-yl)oxy)-3,5-dimethylbenzonitrile (10b)

White solid, 82 % yield, mp 152–154°C. ^{1}H NMR (400 MHz, DMSO-d_6) δ 8.42 (s, 1H, C_6-pyrimidine-H), 7.87 (d, J = 8.0 Hz, 2H), 7.69 (s, 2H), 7.54 (d, J = 8.0 Hz, 2H), 7.16 (s, 1H), 3.50 – 3.42 (m, 2H), 3.20 (s, 3H), 2.74 (s, 2H), 2.07 (s, 6H), 1.90 – 1.16 (m, 7H). ESI-MS: m/z 618.4 $[M + H]^+$. $C_{26}H_{28}IN_5O_3S$ (617.10). HPLC purity: 99.02%.

4-((4-((4-(4-cyano-2,6-dimethylphenoxy)-5-iodopyrimidin-2-yl)amino)piperidin-1-yl)methyl)benzamide (10c)

White solid, 71 % yield, mp 136–138°C. ^{1}H NMR (400 MHz, DMSO-d_6) δ 8.42 (s, 1H, C_6-pyrimidine-H), 7.81 (d, J = 7.9 Hz, 2H), 7.68 (s, 2H), 7.36 – 7.28 (m, 4H), 7.15 (s, 1H), 3.66 – 3.37 (m, 2H), 2.69 (s, 2H), 2.07 (s, 6H), 1.96 – 1.17 (m, 7H). ESI-MS: m/z 583.3 $[M + H]^+$. $C_{26}H_{27}IN_6O_2$ (582.12). HPLC purity: 98.65%.

General procedure for the preparation of intermediates 11-16

$Pd(PPh_3)_4$ (0.05 mmol) and 2M Na_2CO_3 aqueous solution (2.00 mmol) were added to a mixture solution of **10a-c** (1.00 mmol) and boric acid substituents (1.20 mmol) in DMF (10 mL). The mixture was stirred at 100°C for 6-10 h (monitoring with TLC) under N_2. Then the mixture was diluted with 10 mL water, and the aqueous layer was extracted with EtOAc. The organic phase was dried over Na_2SO_4, filtered and evaporated under reduced pressure, purified by flash column chromatography and recrystallized from EA/PE to afford the target compounds **11-16**.

4-((4-((4-(4-cyano-2,6-dimethylphenoxy)-5-(thiophen-2-yl)pyrimidin-2-yl)amino)piperidin-1-yl)methyl)benzenesulfonamide (11a)

11a was synthesized from **10a** (602 mg, 1.0 mmol) and thiophen-2-ylboronic acid (153 mg, 1.2 mmol). White solid, 74% yield, mp 152–153°C. ^{1}H NMR (400 MHz, DMSO-d_6) δ 8.57 (s, 1H, C_6-pyrimidine-H), 7.71 (d, J = 8.0 Hz, 2H, C_3,C_5-Ph-H), 7.63 (s, 2H, C_3,C_5-Ph'-H), 7.52 – 7.43 (m, 3H), 7.39 (d, J = 8.0 Hz, 2H, C_2,C_6-Ph-H), 7.24 (s, 2H, SO_2NH_2), 7.06 – 7.05 (m, 1H), 3.42 (s, 2H, N-CH_2), 2.68 – 2.57 (m, 2H), 2.02 (s, 6H), 1.94 – 1.15 (m, 7H). ^{13}C NMR (100 MHz, DMSO-d_6) δ 163.3, 160.4, 143.1, 135.3, 133.0, 129.4, 127.8, 126.9, 125.9, 123.9, 119.1, 108.7, 62.7, 61.9, 52.6, 31.3, 16.4. ESI-MS: m/z 575.6 $[M + H]^+$, 597.5 $[M + Na]^+$. $C_{29}H_{30}N_6O_3S_2$ (574.18). HPLC purity: 95.98%.

3,5-dimethyl-4-((2-((1-(4-(methylsulfonyl)benzyl)piperidin-4-yl)amino)-5-(thiophen-2-yl)pyrimidin-4-yl)oxy)benzonitrile (11b)

11b was synthesized from **10b** (602 mg, 1.0 mmol) and thiophen-2-ylboronic acid (153 mg, 1.2 mmol). White solid, 82% yield, mp 168–170°C. ^{1}H NMR (400 MHz, DMSO-d_6) δ 8.58 (s, 1H, C_6-pyrimidine-H), 7.81 (d, J = 7.9 Hz, 2H, C_3,C_5-Ph-H), 7.63 (s, 2H, C_3,C_5-Ph'-H), 7.61 – 7.59 (m, 1H), 7.48 (d, J = 7.8 Hz, 2H, C_2,C_6-Ph-H), 7.42 – 7.40 (m, 2H), 7.06 (s, 1H), 3.43 (s, 2H, N-CH_2), 3.13 (s, 3H, SO_2CH_3), 2.68 – 2.60 (m, 2H), 2.02 (s, 6H), 1.94 – 1.24 (m, 7H). ^{13}C NMR (100 MHz, DMSO-d_6) δ 163.3, 160.5, 145.4, 139.8, 135.3, 133.1, 132.5, 129.8, 127.8, 127.4, 125.4, 123.9, 119.1, 61.8, 52.8, 44.0, 31.3, 16.3. ESI-MS: m/z 574.2 $[M + H]^+$, 596.2 $[M + Na]^+$. $C_{30}H_{31}N_5O_3S_2$ (573.19). HPLC purity: 98.32%.

4-((4-((4-(4-cyano-2,6-dimethylphenoxy)-5-(thiophen-2-yl)pyrimidin-2-yl)amino)piperidin-1-yl)methyl)benzamide (11c)

11c was synthesized from **10c** (583 mg, 1.0 mmol) and thiophen-2-ylboronic acid (153 mg, 1.2 mmol). White solid, 70% yield, mp 155–157°C. ^{1}H NMR (400 MHz, DMSO-d_6) δ 8.58 (s, 1H, C_6-pyrimidine-H), 7.85 (s, 1H), 7.75 (d, J = 7.8 Hz, 2H, C_3,C_5-Ph-H), 7.63 (s, 2H, C_3,C_5-Ph'-H), 7.48 – 7.45 (m, 2H), 7.27 (d, J = 7.8 Hz, 2H, C_2,C_6-Ph-H), 7.23 (s, 2H, $CONH_2$), 7.06 (s, 1H), 3.38 (s, 2H, N-CH_2), 2.68 – 2.59 (m, 2H), 2.03 (s, 6H), 1.94 – 1.15 (m, 7H). ^{13}C NMR (100 MHz, DMSO-d_6) δ 168.2, 163.3, 160.4, 142.4, 135.3, 133.4, 133.0, 132.6, 128.9, 127.9, 125.5, 124.0, 121.5, 120.4, 119.1, 108.7, 62.1, 52.7, 31.7, 29.1, 16.3. ESI-MS: m/z 539.7 $[M + H]^+$, 561.1 $[M + Na]^+$. $C_{30}H_{30}N_6O_2S$ (538.22). HPLC purity: 98.29%.

4-((4-((4-(4-cyano-2,6-dimethylphenoxy)-5-(thiophen-3-yl)pyrimidin-2-yl)amino)piperidin-1-yl)methyl)benzenesulfonamide (12a)

12a was synthesized from **10a** (602 mg, 1.0 mmol) and thiophen-3-ylboronic acid (153 mg, 1.2 mmol). White solid, 72% yield, mp 144–146°C. ^{1}H NMR (400 MHz, DMSO-d_6) δ 8.60 (s, 1H, C_6-pyrimidine-H), 7.78 (d, J = 8.0 Hz, 2H, C_3,C_5-Ph-H), 7.67 (s, 2H, C_3,C_5-Ph'-H), 7.62 (s, 2H), 7.46 (d, J = 8.0 Hz, 2H, C_2,C_6-Ph-H), 7.35 – 7.30 (m, 3H), 7.02 (s, 1H, NH), 3.47 (s, 2H, N-CH_2), 2.78 – 2.61 (m, 2H), 2.08 (s, 6H), 1.85 – 1.10 (m, 7H). ^{13}C NMR (100 MHz, DMSO-d_6) δ 164.3, 155.0, 143.3, 133.8, 133.0, 129.4, 126.6, 126.0, 119.1, 108.5, 104.4, 61.9, 60.2, 52.6, 21.2, 16.3, 14.5. ESI-MS: m/z 575.5 $[M + H]^+$, 597.3 $[M + Na]^+$. $C_{29}H_{30}N_6O_3S_2$ (574.18). HPLC purity: 99.11%.

3,5-dimethyl-4-((2-((1-(4-(methylsulfonyl)benzyl)piperidin-4-yl)amino)-5-(thiophen-3-yl)pyrimidin-4-yl)oxy)benzonitrile (12b)

12b was synthesized from **10b** (602 mg, 1.0 mmol) and thiophen-3-ylboronic acid (153 mg, 1.2 mmol). White solid, 66% yield, mp 159–161°C. ^{1}H NMR (400 MHz, DMSO-d_6) δ 8.60 (s, 1H, C_6-pyrimidine-H), 7.88 (d, J = 7.9 Hz, 2H, C_3,C_5-Ph-H), 7.83 – 7.68 (m, 1H), 7.62 (s, 2H, C_3,C_5-Ph'-H), 7.67 – 7.60 (m, 2H), 7.55 (d, J = 8.0 Hz, 2H, C_2,C_6-Ph-H), 7.02 (s, 1H, NH), 3.43 (s, 2H, N-CH_2), 3.20 (s, 3H, SO_2CH_3), 2.86 – 2.58 (m, 2H), 2.08 (s, 6H), 1.94 – 1.17 (m, 7H). ^{13}C NMR (100 MHz, DMSO-d_6) δ 164.1, 155.2, 145.1, 143.6, 139.0, 133.3, 132.4, 129.7, 127.8, 119.1, 118.2, 108.6, 61.9, 52.7, 44.0, 31.3, 16.2. ESI-MS: m/z 574.3 $[M + H]^+$, 596.6 $[M + Na]^+$. $C_{30}H_{31}N_5O_3S_2$ (573.19). HPLC purity: 98.66%.

4-((4-((4-(4-cyano-2,6-dimethylphenoxy)-5-(thiophen-3-yl)pyrimidin-2-yl)amino)piperidin-1-yl)methyl)benzamide (12c)

12c was synthesized from **10c** (583 mg, 1.0 mmol) and thiophen-3-ylboronic acid (153 mg, 1.2 mmol). White solid, 74% yield, mp 140–142°C. ^{1}H NMR (400 MHz, DMSO-d_6) δ 8.60 (s, 1H, C_6-pyrimidine-H), 7.92 (s, 1H), 7.82 (d, J = 8.0 Hz, 2H, C_3,C_5-Ph-H), 7.68 (s, 2H, C_3,C_5-Ph'-H), 7.62 (s, 2H), 7.33 (d, J = 7.9 Hz, 2H, C_2,C_6-Ph-H), 7.30 (s, 2H, $CONH_2$), 7.02 (s, 1H), 3.44 (s, 2H, N-CH_2), 2.64 – 2.59 (m, 2H), 2.09 (s, 6H), 2.00 – 1.20 (m, 7H). ^{13}C NMR (100 MHz, DMSO-d_6) δ 164.2, 155.0, 143.7, 140.2, 133.1, 131.9, 129.1, 126.5, 122.8, 121.4, 119.8, 118.2, 115.8, 108.0, 61.9, 60.2, 52.5, 21.2, 16.3, 14.5. ESI-MS: m/z 539.4 $[M + H]^+$, 561.3 $[M + Na]^+$. $C_{30}H_{30}N_6O_2S$ (538.22). HPLC purity: 96.59%.

4-((4-((4-(4-cyano-2,6-dimethylphenoxy)-5-(furan-2-yl)pyrimidin-2-yl)amino) piperidin-1-yl)methyl)benzenesulfonamide (13a)

13a was synthesized from **10a** (602 mg, 1.0 mmol) and furan-2-ylboronic acid (134 mg, 1.2 mmol). White solid, 77% yield, mp 140–142°C. ^{1}H NMR (400 MHz, DMSO-d_6) δ 8.61 (s, 1H, C_6-pyrimidine-H), 7.78 (d, J = 7.9 Hz, 2H, C_3,C_5-Ph-H), 7.77 – 7.70 (m, 2H), 7.72 (s, 2H, C_3,C_5-Ph'-H), 7.46 (d, J = 8.0 Hz, 2H, C_2,C_6-Ph-H), 7.31 – 7.19 (m, 3H), 6.59 (s, 1H, NH), 3.47 (s, 2H, N-CH_2), 2.51 – 2.02 (m, 2H), 2.02 (s, 6H), 1.95 – 1.13 (m, 7H). ^{13}C NMR (100 MHz, DMSO-d_6) δ 170.8, 163.0, 160.2, 156.3, 147.1, 143.2, 142.1, 133.1, 129.4, 126.9, 126.0, 119.1, 112.3, 108.7, 61.9, 60.2, 52.7, 21.2, 16.1. ESI-MS: m/z 559.4 $[M + H]^+$, 581.4 $[M + Na]^+$. $C_{29}H_{30}N_6O_4S$ (558.20). HPLC purity: 98.96%.

4-((5-(furan-2-yl)-2-((1-(4-(methylsulfonyl)benzyl)piperidin-4-yl)amino) pyrimidin-4-yl)oxy)-3,5-dimethylbenzonitrile (13b)

13b was synthesized from **10b** (602 mg, 1.0 mmol) and furan-2-ylboronic acid (134 mg, 1.2 mmol). White solid, 82% yield, mp 137–139°C. ^{1}H NMR (400 MHz, DMSO-d_6) δ 8.60 (s, 1H, C_6-pyrimidine-H), 7.88 (d, J = 7.9 Hz, 2H, C_3,C_5-Ph-H), 7.72 – 7.63 (m, 3H), 7.55 (d, J = 7.8 Hz, 2H, C_2,C_6-Ph-H), 6.73 (d, J = 11.7 Hz, 1H), 7.21 – 7.19 (m, 1H), 6.59 (s, 1H, NH), 3.51 (s, 2H, N-CH_2), 3.20 (s, 3H, SO_2CH_3), 2.83 – 2.57 (m, 2H), 2.02 (s, 6H), 1.94 – 1.18 (m, 7H). ^{13}C NMR (100 MHz, DMSO-d_6) δ 163.0, 160.3, 156.0, 147.1, 145.3, 142.1, 139.8, 133.1, 132.5, 129.8, 128.5, 127.4, 119.1, 112.3, 107.7, 61.8, 52.7, 44.0, 31.2, 16.3. ESI-MS: m/z 558.6 $[M + H]^+$, 580.4 $[M + Na]^+$. $C_{30}H_{31}N_5O_4S$ (557.21). HPLC purity: 97.52%.

4-((4-((4-(4-cyano-2,6-dimethylphenoxy)-5-(furan-2-yl)pyrimidin-2-yl)amino)piperidin-1-yl)methyl)benzamide (13c)

13c was synthesized from **10c** (583 mg, 1.0 mmol) and furan-2-ylboronic acid (134 mg, 1.2 mmol). White solid, 65% yield, mp 148–150°C. ^{1}H NMR (400 MHz, DMSO-d_6) δ 8.60 (s, 1H, C_6-pyrimidine-H), 7.91 (s, 1H), 7.82 (d, J = 7.8 Hz, 2H, C_3,C_5-Ph-H), 7.71 (s, 2H, C_3,C_5-Ph'-H), 7.52 (s, 1H), 7.41 – 7.14 (m, 4H), 6.73 (d, J = 12.4 Hz, 1H), 6.58 (s, 1H, NH), 3.38 (s, 2H, N-CH_2), 2.89 – 2.60 (m, 2H), 2.03 (s, 6H), 1.94 – 1.14 (m, 7H). ^{13}C NMR (100 MHz, DMSO-d_6) δ 168.2, 163.0, 160.2, 154.2, 147.1, 142.1, 133.4, 133.0, 132.5, 128.9, 127.9, 119.1, 112.3, 108.7, 100.6, 62.1, 52.5, 31.2, 16.0. ESI-MS: m/z 523.3 $[M + H]^+$. $C_{30}H_{30}N_6O_3$ (522.24). HPLC purity: 97.49%.

4-((4-((4-(4-cyano-2,6-dimethylphenoxy)-5-(furan-3-yl)pyrimidin-2-yl)amino) piperidin-1-yl)methyl)benzenesulfonamide (14a)

14a was synthesized from **10a** (602 mg, 1.0 mmol) and furan-3-ylboronic acid (134 mg, 1.2 mmol). White solid, 69% yield, mp 172–174°C. ^{1}H NMR (400 MHz, DMSO-d_6) δ 8.52 (s, 1H, C_6-pyrimidine-H), 8.00 (s, 1H), 7.85 (s, 1H), 7.75 (d, J = 7.8 Hz, 2H, C_3,C_5-Ph-H), 7.68 (s, 1H), 7.62 (s, 2H, C_3,C_5-Ph'-H), 7.30 – 7.19 (m, 4H), 7.00 (s, 1H, NH), 3.39 – 3.32 (m, 2H, N-CH_2), 2.77 – 2.52 (m, 2H), 2.01 (s, 6H), 1.81 – 1.07 (m, 7H). ^{13}C NMR (100 MHz, DMSO-d_6) δ 168.2, 164.2, 160.4, 143.9, 140.0, 133.4, 133.1, 132.6, 128.9, 127.9,126.0, 119.1, 118.2, 108.9, 108.5, 62.1, 52.6, 39.4, 31.4, 16.2. ESI-MS: m/z 559.3 $[M + H]^+$, 581.4 $[M + Na]^+$. $C_{29}H_{30}N_6O_4S$ (558.20). HPLC purity: 98.96%.

4-((5-(furan-3-yl)-2-((1-(4-(methylsulfonyl)benzyl)piperidin-4-yl)amino) pyrimidin-4-yl)oxy)-3,5-dimethylbenzonitrile (14b)

14b was synthesized from **10b** (602 mg, 1.0 mmol) and furan-3-ylboronic acid (134 mg, 1.2 mmol). White solid, 77% yield, mp 180–182°C. ^{1}H NMR (400 MHz, DMSO-d_6) δ 8.52 (s, 1H, C_6-pyrimidine-H), 8.01 (s, 1H), 7.81 (d, J = 7.9 Hz, 2H, C_3,C_5-Ph-H), 7.70 – 7.66 (m, 1H), 7.62 (s, 2H, C_3,C_5-Ph'-H), 7.48 (d, J = 7.9 Hz, 2H, C_2,C_6-Ph-H), 7.27 (s, 1H), 7.00 (s, 1H, NH), 3.44 (s, 2H, N-CH_2), 3.13 (s, 3H, SO_2CH_3), 2.75 –2.63 (m, 2H), 2.01 (s, 6H), 1.90 – 1.28 (m, 7H). ^{13}C NMR (100 MHz, DMSO-d_6) δ 164.2, 145.4, 143.9, 140.0, 139.8, 133.1, 132.6, 129.7, 127.4, 119.1, 118.2, 108.8, 61.9, 52.7, 44.0, 31.4, 16.2. ESI-MS: m/z 558.5 $[M + H]^+$, 580.2 $[M + Na]^+$. $C_{30}H_{31}N_5O_4S$ (557.21). HPLC purity: 99.01%.

4-((4-((4-(4-cyano-2,6-dimethylphenoxy)-5-(furan-3-yl)pyrimidin-2-yl)amino) piperidin-1-yl)methyl)benzamide (14c)

14c was synthesized from **10c** (583 mg, 1.0 mmol) and furan-3-ylboronic acid (134 mg, 1.2 mmol). White solid, 71% yield, mp 158–160°C. ^{1}H NMR (400 MHz, DMSO-d_6) δ 8.52 (s, 1H, C_6-pyrimidine-H), 8.00 (s, 1H), 7.76 – 7.68 (m, 4H), 7.62 (s, 2H), 7.39 (d, J = 7.9 Hz, 2H, C_2,C_6-Ph-H), 7.24 (s, 2H), 7.00 (s, 1H, NH), 3.39 (s, 2H, N-CH_2), 2.81 – 2.53 (m, 2H), 2.01 (s, 6H), 1.96 – 1.19 (m, 7H). ^{13}C NMR (100 MHz, DMSO-d_6) δ 164.2, 143.9, 143.1, 140.0, 133.1, 132.4, 129.4, 126.0, 123.0, 121.9, 119.1, 118.2, 115.8, 108.8, 61.9, 60.2, 52.6, 21.2, 16.2, 14.5. ESI-MS: m/z 523.3 $[M + H]^+$, 545.4 $[M + Na]^+$. $C_{30}H_{30}N_6O_3$ (522.24). HPLC purity: 97.48%.

4-((4-((4-(4-cyano-2,6-dimethylphenoxy)-5-phenylpyrimidin-2-yl)amino) piperidin-1-yl)methyl)benzenesulfonamide (15a)

15a was synthesized from **10a** (602 mg, 1.0 mmol) and phenylboronic acid (145 mg, 1.2 mmol). White solid, 79% yield, mp 162–164°C. ^{1}H NMR (400 MHz, DMSO-d_6) δ 8.34 (s, 1H, C_6-pyrimidine-H), 7.78 (d, J = 8.0 Hz, 2H, C_3,C_5-Ph-H), 7.64 (s, 2H, C_3,C_5-Ph'-H), 7.64 – 7.49 (m, 3H), 7.45 – 7.39 (m, 3H), 7.32 (d, J = 8.0 Hz, 2H, C_2,C_6-Ph-H), 7.05 (s, 1H), 3.47 (s, 2H, N-CH_2), 2.89 – 2.59 (m, 2H), 2.08 (s, 6H), 1.87 – 1.15 (m, 7H). ^{13}C NMR (100 MHz, DMSO) δ 164.7, 161.0, 156.2, 154.4, 143.4, 143.1, 133.0, 132.5, 129.4, 129.0, 128.6, 127.3, 126.0, 119.1, 115.7, 112.4, 108.6, 62.0, 60.2, 52.7, 21.2, 16.4, 14.5. ESI-MS: m/z 569.2 $[M + H]^+$. $C_{31}H_{32}N_6O_3S$ (568.23). HPLC purity: 96.98%.

3,5-dimethyl-4-((2-((1-(4-(methylsulfonyl)benzyl)piperidin-4-yl)amino)-5-phenylpyrimidin-4-yl)oxy)benzonitrile (15b)

15b was synthesized from **10b** (602 mg, 1.0 mmol) and phenylboronic acid (145 mg, 1.2 mmol). White solid, 81% yield, mp 147–149°C. ^{1}H NMR (400 MHz, DMSO-d_6) δ 8.27 (s, 1H, C_6-pyrimidine-H), 7.81 (d, J = 8.0 Hz, 2H, C_3,C_5-Ph-H), 7.64 – 7.53 (m, 4H), 7.48 (d, J = 7.9 Hz, 2H, C_2,C_6-Ph-H), 7.38 (t, J = 7.7 Hz, 2H), 7.26 (t, J = 7.6 Hz, 1H), 6.97 (s, 1H), 3.54 – 3.35 (m, 2H, N-CH_2), 3.13 (s, 3H, SO_2CH_3), 2.68 – 2.62 (m, 2H), 2.01 (s, 6H), 1.90 – 1.17 (m, 7H). ^{13}C NMR (100 MHz, DMSO) δ 164.3, 156.0, 153.8, 143.7, 142.8, 133.7, 132.5, 129.0, 128.6, 127.3, 125.2, 118.4, 115.6, 112.7, 108.0, 62.1, 52.7, 21.4, 16.3, 14.5. ESI-MS: m/z 568.4 $[M + H]^+$, 590.5 $[M + Na]^+$. $C_{32}H_{33}N_5O_3S$ (567.23). HPLC purity: 98.59%.

4-((4-((4-(4-cyano-2,6-dimethylphenoxy)-5-phenylpyrimidin-2-yl)amino) piperidin-1-yl)methyl)benzamide (15c)

15c was synthesized from **10c** (583 mg, 1.0 mmol) and phenylboronic acid (145 mg, 1.2 mmol). White solid, 64% yield, mp 150–152°C. ^{1}H NMR (400 MHz, DMSO-d_6) δ 8.34 (s, 1H, C_6-pyrimidine-H), 7.92 (s, 1H), 7.83 (d, J = 7.8 Hz, 2H, C_3,C_5-Ph-H), 7.65 (d, J = 12.5 Hz, 4H), 7.45 (t, J = 7.6 Hz, 2H), 7.37 – 7.27 (m, 4H), 7.04 (s, 1H, NH), 3.38 (s, 2H, N-CH_2), 2.73 – 2.57 (m, 2H), 2.08 (s, 6H), 2.02 – 1.17 (m, 7H). ^{13}C NMR (100 MHz, DMSO-d_6) δ 164.2, 155.7, 152.6, 143.7, 142.4, 133.1, 131.7, 129.3, 125.8, 122.3, 119.3, 118.2, 115.8, 108.0, 61.7, 60.2, 52.5, 21.2, 16.4, 14.5. ESI-MS: m/z 533.7 $[M + H]^+$, 555.2 $[M + Na]^+$. $C_{32}H_{32}N_6O_2$ (532.26). HPLC purity: 98.96%.

4-((4-((4-(4-cyano-2,6-dimethylphenoxy)-5-(pyridin-4-yl)pyrimidin-2-yl)amino) piperidin-1-yl)methyl)benzenesulfonamide (16a)

16a was synthesized from **10a** (602 mg, 1.0 mmol) and pyridin-4-ylboronic acid (145 mg, 1.2 mmol). White solid, 53% yield, mp 174–176°C. ^{1}H NMR (400 MHz, DMSO-d_6) δ 8.60 – 8.54 (m, 3H), 8.18 (d, J = 5.4 Hz, 2H), 7.76 – 7.73 (m, 2H), 7.64 (s, 2H, C_3,C_5-Ph'-H), 7.46 (d, J = 8.0 Hz, 2H), 7.31 (s, 2H), 6.95 (s, 1H, NH), 3.47 (s, 2H, N-CH_2), 2.87 – 2.59 (m, 2H), 2.09 (s, 6H), 2.03 – 1.22 (m, 7H). ^{13}C NMR (100 MHz, DMSO) δ 164.5, 161.4, 156.4, 143.7, 143.0, 133.6, 129.4, 129.0, 128.5, 128.1, 127.3, 126.2, 119.0, 118.2, 115.7, 112.9, 108.3, 62.0, 60.7, 52.7, 21.2, 16.4, 14.5. ESI-MS: m/z 570.3 $[M + H]^+$, 592.1 $[M + Na]^+$. $C_{30}H_{31}N_7O_3S$ (569.22). HPLC purity: 99.32%.

3,5-dimethyl-4-((2-((1-(4-(methylsulfonyl)benzyl)piperidin-4-yl)amino)-5-(pyridin-4-yl)pyrimidin-4-yl)oxy)benzonitrile (16b)

16b was synthesized from **10b** (602 mg, 1.0 mmol) and pyridin-4-ylboronic acid (145 mg, 1.2 mmol). White solid, 59% yield, mp 158–160°C. ^{1}H NMR (400 MHz, DMSO-d_6) δ 8.60 (d, J = 5.1 Hz, 2H), 8.55 (d, J = 6.2 Hz, 1H), 7.88 (d, J = 7.9 Hz, 2H), 7.74 (d, J = 5.1 Hz, 1H), 7.69 (s, 3H), 7.55 (d, J = 7.9 Hz, 2H), 7.04 (s, 1H), 3.55 – 3.48 (m, 2H, N-CH_2), 3.20 (s, 3H), 2.92 – 2.60 (m, 2H), 2.09 (s, 6H), 2.02 – 1.22 (m, 7H). ^{13}C NMR (100 MHz, DMSO) δ 164.2, 160.7, 156.9, 153.8, 143.7, 142.1, 133.7, 132.5, 128.2, 127.9, 125.8, 119.3, 118.3, 115.0, 112.7, 108.0, 62.3, 52.7, 21.4, 16.4, 14.5. ESI-MS: m/z 569.2 $[M + H]^+$, 591.5 $[M + Na]^+$. $C_{31}H_{32}N_6O_3S$ (568.23). HPLC purity: 97.65%.

4-((4-((4-(4-cyano-2,6-dimethylphenoxy)-5-(pyridin-4-yl)pyrimidin-2-yl)amino) piperidin-1-yl)methyl)benzamide (16c)

16c was synthesized from **10c** (583 mg, 1.0 mmol) and pyridin-4-ylboronic acid (145 mg, 1.2 mmol). White solid, 52% yield, mp 163–165°C. ^{1}H NMR (400 MHz, DMSO-d_6) δ 8.61 – 8.53 (m, 3H), 7.87 (d, J = 7.8 Hz, 2H), 7.74 – 7.67 (m, 4H), 7.69 (s, 2H), 7.55 (d, J = 7.9 Hz, 2H), 7.04 (s, 1H), 3.50 – 3.48 (m, 2H, N-CH_2), 2.75 – 2.61 (m, 2H), 2.08 (s, 6H), 2.02 – 1.29 (m, 7H). ^{13}C NMR (100 MHz, DMSO-d_6) δ 164.3, 160.1, 155.8, 152.6, 143.6, 142.3, 133.7, 132.1, 129.2, 127.4, 125.1, 122.2, 119.0, 118.5, 115.8, 108.7, 61.5, 60.2, 52.5, 21.2, 16.4, 14.5. ESI-MS: m/z 534.7 $[M + H]^+$, 556.4 $[M + Na]^+$. $C_{31}H_{31}N_7O_2$ (533.25). HPLC purity: 98.78%.

(*E*)-3-(4-((2-chloropyrimidin-4-yl)oxy)-3,5-dimethylphenyl)acrylonitrile (17)

The synthetic method was similar to that described for **6**, except that the starting material **5** (1.50 g, 10 mmol) was reacted with (*E*)-3-(4-hydroxy-3,5-dimethylphenyl)acrylonitrile (2.07 g, 12 mmol). White solid, 84 % yield. ^{1}H NMR (400 MHz, DMSO-d_6) δ 8.67 (d, J = 5.7 Hz, 1H), 7.62 (d, J = 16.7 Hz, 1H), 7.52 (s, 2H), 7.25 (d, J = 5.7 Hz, 1H), 6.45 (d, J = 16.7 Hz, 1H), 2.07 (s, 6H). ESI-MS: m/z 286.2 $[M + H]^+$. $C_{15}H_{12}ClN_3O$ (285.07). HPLC purity: 98.39%.

tert-butyl(*E*)-4-((4-(4-(2-cyanovinyl)-2,6-dimethylphenoxy)pyrimidin-2-yl) amino)piperidine-1-carboxylate (18)

The synthetic method was similar to that described for **7**, except that the starting material **17** (0.28 g, 1.0 mmol) was reacted with *N*-Boc-4-aminopiperidine (0.24 g, 1.2 mmol). White solid, 70% yield. ^{1}H NMR (400 MHz, DMSO-d_6) δ 8.17 (d, J = 5.6 Hz, 1H), 7.68 – 7.51 (m, 1H), 7.46 (d, J = 4.5 Hz, 2H), 6.40 (d, J = 16.6 Hz, 1H), 6.17 (s, 1H), 3.85 (s, 3H), 2.81 (d, J = 63.8 Hz, 2H), 2.06 (s, 6H), 1.91 – 1.52 (m, 3H), 1.41 (d, J = 6.0 Hz, 3H), 1.38 (s, 6H), 1.31 – 0.99 (m, 2H). ESI-MS: m/z 472.02 $[M + Na]^+$. $C_{25}H_{31}N_5O_3$ (449.24). HPLC purity: 98.79%.

tert-butyl(*E*)-4-((4-(4-(2-cyanovinyl)-2,6-dimethylphenoxy)-5-iodopyrimidin-2-yl)amino)piperidine-1-carboxylate (19)

The synthetic method was similar to that described for **8**, except that NIS (0.34 g, 1.5 mmol) was reacted with **18** (0.47 g, 1.0 mmol). White solid, 79% yield. ESI-MS: m/z 576.2 $[M + H]^+$. $C_{25}H_{30}IN_5O_3$ (575.14). HPLC purity: 96.28%.

(*E*)-3-(4-((5-iodo-2-(piperidin-4-ylamino)pyrimidin-4-yl)oxy)-3,5-dimethylphenyl)acrylonitrile (20)

The synthetic method was similar to that described for **9**. White solid, 85% yield. ^{1}H NMR (400 MHz, DMSO-d_6) δ 8.45 (s, 1H, C_6-pyrimidine-H), 8.27 (s, 1H), 7.60 (d, J = 16.6 Hz, 1H, ArCH=), 7.47 (s, 2H), 7.32 (d, J = 13.5 Hz, 1H), 6.42 (d, J = 16.7 Hz, 1H, =CHCN), 3.23 – 2.71 (m, 5H), 2.06 (s, 6H), 1.94 – 1.26 (m, 4H). ESI-MS: m/z 476.2 $[M + H]^+$, 498.5 $[M + Na]^+$. $C_{20}H_{22}IN_5O$ (475.09). HPLC purity: 97.09%.

(*E*)-4-((4-((4-(4-(2-cyanovinyl)-2,6-dimethylphenoxy)-5-iodopyrimidin-2-yl) amino)piperidin-1-yl)methyl)benzenesulfonamide (21a)

The synthetic method was similar to that described for **10a-c**. White solid, 75% yield, mp: 210-212°C. ^{1}H NMR (400 MHz, DMSO-d_6) δ 8.41 (s, 1H, C_6-pyrimidine-H), 7.96 (s, 1H), 7.77 (d, J = 7.9 Hz, 2H), 7.68 – 7.55 (m, 2H), 7.46 (s, 2H), 7.35 – 7.26 (m, 2H), 7.15 (s, 1H, NH), 6.42 (d, J = 16.7 Hz, 1H, =CHCN), 3.41 (s, 2H, N-CH_2), 2.74 (s, 2H), 2.04 (s, 6H), 1.86 – 1.08 (m, 7H). ESI-MS: m/z 645.7 $[M + H]^+$, 667.2 $[M + Na]^+$. $C_{27}H_{29}IN_6O_3S$ (644.11). HPLC purity: 96.59%.

(*E*)-3-(4-((5-iodo-2-((1-(4-(methylsulfonyl)benzyl)piperidin-4-yl)amino) pyrimidin-4-yl)oxy)-3,5-dimethylphenyl)acrylonitrile (21b)

The synthetic method was similar to that described for **10a-c**. White solid, 82% yield, mp: 204-206°C. ^{1}H NMR (400 MHz, DMSO-d_6) δ 8.41 (s, 1H, C_6-pyrimidine-H), 7.88 (d, J = 8.1 Hz, 2H), 7.68 – 7.58 (m, 2H), 7.45 (s, 2H), 7.29 – 7.27 (m, 1H), 7.15 (s, 1H, NH), 6.41 (d, J = 16.7 Hz, 1H, =CHCN), 3.47 – 3.45 (m, 2H), 3.20 (s, 3H, SO_2CH_3), 2.74 (s, 2H), 2.04 (s, 6H), 1.83 – 1.10 (m, 7H). ESI-MS: m/z 644.5 $[M + H]^+$, 666.3 $[M + Na]^+$. $C_{28}H_{30}IN_5O_3S$ (643.11). HPLC purity: 99.02%.

(*E*)-4-((4-((4-(4-(2-cyanovinyl)-2,6-dimethylphenoxy)-5-iodopyrimidin-2-yl) amino)piperidin-1-yl)methyl)benzamide (21c)

The synthetic method was similar to that described for **10a-c**. White solid, 74% yield, mp: 231-232°C. [1] ^{1}H NMR (400 MHz, DMSO-d_6) δ 8.40 (s, C_6-pyrimidine-H), 7.91 (s, 1H), 7.81 (d, J = 7.9 Hz, 2H), 7.45 (s, 2H), 7.38 – 7.08 (m, 5H), 6.42 (d, J = 16.5 Hz, 1H, =CHCN), 3.54 – 3.47 (m, 2H), 2.74 (s, 2H), 2.04 (s, 6H), 1.99 – 1.21 (m, 7H). ESI-MS: m/z 609.2 $[M + H]^+$, 631.4 $[M + Na]^+$. $C_{28}H_{29}IN_6O_2$ (608.14). HPLC purity: 99.25%.

(*E*)-4-((4-((4-(4-(2-cyanovinyl)-2,6-dimethylphenoxy)-5-(pyridin-4-yl)pyrimidin-2-yl)amino)piperidin-1-yl)methyl)benzenesulfonamide (22a)

22a was synthesized from **21a** (644 mg, 1.0 mmol) and pyridin-4-ylboronic acid (145 mg, 1.2 mmol). White solid, 59% yield, mp: 134-136°C. ^{1}H NMR (400 MHz, DMSO-d_6) δ 8.53 (s, 1H, C_6-pyrimidine-H), 8.46 (d, J = 6.6 Hz, 2H), 7.71 (d, J = 8.1 Hz, 2H), 7.65 – 7.47 (m, 3H), 7.39 – 7.35 (m, 3H), 7.24 – 7.21 (m, 3H), 6.91 (s, 1H, NH), 6.35 (d, J = 17.3 Hz, 1H, =CHCN), 3.43 (s, 2H, N-CH_2), 2.88 – 2.47 (m, 2H), 1.99 (s, 6H), 1.87 – 1.09 (m, 7H). ^{13}C NMR (100 MHz, DMSO-d_6): δ 170.6, 165.3, 161.6, 160.4, 150.7, 150.4, 143.2, 131.6, 129.5, 128.6, 128.1, 126.0, 123.0, 122.5, 119.4, 96.6, 90.8, 62.1, 52.8, 50.6, 31.6, 29.0, 16.5. ESI-MS: m/z 596.3 $[M + H]^+$, 618.5 $[M + Na]^+$. $C_{32}H_{33}N_7O_3S$ (595.24). HPLC purity: 97.19%.

(*E*)-3-(3,5-dimethyl-4-((2-((1-(4-(methylsulfonyl)benzyl)piperidin-4-yl)amino)-5-(pyridin-4-yl)pyrimidin-4-yl)oxy)phenyl)acrylonitrile (22b)

22b was synthesized from **21b** (643 mg, 1.0 mmol) and pyridin-4-ylboronic acid (145 mg, 1.2 mmol). White solid, 63% yield, mp: 122-124°C. ^{1}H NMR (400 MHz, DMSO-d_6) δ 8.75 – 8.47 (m, 3H), 7.88 (d, J = 7.8 Hz, 2H), 7.75 – 7.69 (m, 2H), 7.66 – 7.49 (m, 3H), 7.46 (s, 2H), 6.91 (s, 1H, NH), 6.41 (d, J = 16.9 Hz, 1H, =CHCN), 3.48 – 3.45 (m, 2H, N-CH_2), 3.20 (s, 3H, SO_2CH_3), 2.94 – 2.54 (m, 2H), 2.07 (s, 6H), 2.00 – 1.17 (m, 7H). ^{13}C NMR (100 MHz, DMSO-d_6) δ 168.8, 165.2, 161.5, 150.6, 150.2, 145.5, 139.8, 131.6, 131.3, 129.7, 128.6, 128.2, 127.4, 122.6, 119.4, 105.6, 61.9, 52.8, 44.0, 31.7, 29.0, 16.6. ESI-MS: m/z 595.5 $[M + H]^+$. $C_{33}H_{34}N_6O_3S$ (594.2). HPLC purity: 98.54%.

(*E*)-4-((4-((4-(4-(2-cyanovinyl)-2,6-dimethylphenoxy)-5-(pyridin-4-yl)pyrimidin-2-yl)amino)piperidin-1-yl)methyl)benzamide (22c)

22c was synthesized from **21c** (608 mg, 1.0 mmol) and pyridin-4-ylboronic acid (145 mg, 1.2 mmol). White solid, 50% yield, mp: 125-127°C. ^{1}H NMR (400 MHz, DMSO-d_6) δ 8.52 (s, 1H, C_6-pyrimidine-H), 8.46 (d, J = 6.0 Hz, 2H), 7.85 (s, 1H), 7.76 (d, J = 7.7 Hz, 2H), 7.70 – 7.47 (m, 3H), 7.39 (s, 2H), 7.32 – 7.18 (m, 3H), 6.90 (s, 1H, NH), 6.34 (d, J = 16.7 Hz, 1H, =CHCN), 3.41 (s, 2H, N-CH_2), 2.73 (s, 2H), 1.99 (s, 6H), 1.77 – 1.15 (m, 7H). ^{13}C NMR (100 MHz, DMSO-d_6) δ 168.2, 161.6, 150.2, 142.5, 133.5, 131.7, 131.6, 128.9, 128.8, 127.9, 122.9, 122.6, 119.4, 96.5, 62.1, 52.8, 31.7, 29.0, 16.5. ESI-MS: m/z 560.3 $[M + H]^+$, 682.4 $[M + Na]^+$. $C_{33}H_{33}N_7O_2$ (559.27). HPLC purity: 97.44%.

(*E*)-4-((4-((4-(4-(2-cyanovinyl)-2,6-dimethylphenoxy)-5-(2-methoxypyridin-4-yl)pyrimidin-2-yl)amino)piperidin-1-yl)methyl)benzenesulfonamide (23a)

23a was synthesized from **21a** (644 mg, 1.0 mmol) and (2-methoxypyridin-4-yl)boronic acid (183 mg, 1.2 mmol). White solid, 65% yield, mp: 132-134°C. ^{1}H NMR (400 MHz, DMSO-d_6) δ 8.51 (d, J = 6.1 Hz, 1H), 8.19 (d, J = 5.4 Hz, 1H), 7.78 (d, J = 7.7 Hz, 2H), 7.59 (d, J = 15.4 Hz, 1H, ArCH=), 7.46 – 7.42 (m, 5H), 7.37 –7.30 (m, 3H), 7.14 (s, 1H, NH), 6.50 – 6.34 (m, 1H, =CHCN), 3.88 (s, 3H, OCH_3), 3.44 (s, 2H, N-CH_2), 2.77 – 2.74 (m, 2H), 2.06 (s, 6H), 1.99 – 1.17 (m, 7H). ^{13}C NMR (100 MHz, DMSO-d_6) δ 168.7, 164.5, 161.5, 155.2, 150.7, 147.3, 147.3, 143.4, 143.1, 131.6, 129.4, 128.6, 128.2, 126.0, 119.4, 116.9, 116.5, 109.1, 108.7, 96.4, 62.0, 53.5, 52.6, 31.2, 16.5. ESI-MS: m/z 626.4 $[M + H]^+$, 643.7 $[M + NH_4]^+$. $C_{33}H_{35}N_7O_4S$ (625.25). HPLC purity: 98.55%.

(*E*)-3-(4-((5-(2-methoxypyridin-4-yl)-2-((1-(4-(methylsulfonyl)benzyl)piperidin-4-yl)amino)pyrimidin-4-yl)oxy)-3,5-dimethylphenyl)acrylonitrile (23b)

23b was synthesized from **21b** (643 mg, 1.0 mmol) and (2-methoxypyridin-4-yl)boronic acid (183 mg, 1.2 mmol). White solid, 65% yield, mp: 225-227°C. ^{1}H NMR (400 MHz, DMSO-d_6) δ 8.51 (d, J = 6.1 Hz, 1H), 8.24 – 8.11 (m, 1H), 7.88 (d, J = 7.8 Hz, 2H), 7.68 – 7.49 (m, 4H), 7.45 (d, J = 5.2 Hz, 2H), 7.36 – 7.29 (m, 1H), 7.13 (s, 1H, NH), 6.40 (d, J = 16.7, 1H, =CHCN), 3.87 (s, 3H, OCH_3), 3.54 (s, 2H, N-CH_2), 3.20 (s, 3H, SO_2CH_3), 2.75 – 2.60 (m, 2H), 2.05 (s, 6H), 1.96 – 1.12 (m, 7H). ^{13}C NMR (100 MHz, DMSO-d_6) δ 168.7, 164.4, 161.6, 147.3, 145.5, 139.8, 137.4, 131.5, 129.7, 127.4, 119.4, 116.5, 108.7, 96.4, 61.9, 53.5, 52.6, 44.0, 31.7, 29.0, 16.7. ESI-MS: m/z 625.3 $[M + H]^+$. $C_{34}H_{36}N_6O_4S$ (624.25). HPLC purity: 97.90%.

(*E*)-4-((4-((4-(4-(2-cyanovinyl)-2,6-dimethylphenoxy)-5-(2-methoxypyridin-4-yl)pyrimidin-2-yl)amino)piperidin-1-yl)methyl)benzamide (23c)

23c was synthesized from **21c** (608 mg, 1.0 mmol) and (2-methoxypyridin-4-yl)boronic acid (183 mg, 1.2 mmol). White solid, 72% yield, mp: 170-172°C. ^{1}H NMR (400 MHz, DMSO-d_6) δ 8.51– 8.37 (m, 2H), 7.80 (d, J = 7.8 Hz, 2H), 7.59 (d, J = 16.4 Hz, 1H, ArCH=), 7.45 – 7.42 (m, 3H), 7.40 – 7.39 (m, 2H), 7.37 –7.30 (m, 3H), 7.14 (s, 1H, NH), 6.44 (d, J = 16.7 Hz, 1H, =CHCN), 3.87 (s, 3H, OCH_3), 3.43 (s, 2H, N-CH_2), 2.73 – 2.71 (m, 2H), 2.04 (s, 6H), 1.99 – 1.21 (m, 7H). ^{13}C NMR (100 MHz, DMSO-d_6) δ 168.7, 154.5, 161.7, 155.2, 150.7, 147.5, 147.3, 143.4, 142.8, 131.6, 129.4, 128.6, 128.0, 126.5, 119.4, 116.8, 109.1, 108.7, 96.4, 62.2, 53.5, 52.6, 31.5, 16.7. ESI-MS: m/z 590.2 $[M + H]^+$, 612.4 $[M + Na]^+$. $C_{34}H_{35}N_7O_3$ (589.28). HPLC purity: 98.11%.

(*E*)-4-((4-((4-(4-(2-cyanovinyl)-2,6-dimethylphenoxy)-5-(2-methylpyridin-4-yl)pyrimidin-2-yl)amino)piperidin-1-yl)methyl)benzenesulfonamide (24a)

24a was synthesized from **21a** (644 mg, 1.0 mmol) and (2-methylpyridin-4-yl)boronic acid (164 mg, 1.2 mmol). White solid, 57% yield, mp: 138-140°C. ^{1}H NMR (400 MHz, DMSO-d_6) δ 8.40 (dd, J = 13.9, 7.8 Hz, 2H), 7.71 (d, J = 7.7 Hz, 2H), 7.58 – 7.40 (m, 3H), 7.38 (d, J = 6.5 Hz, 4H), 7.24 (d, J = 5.2 Hz, 2H), 6.88 (s, 1H, NH), 6.34 (d, J = 17.3, 1H, =CHCN), 3.43 (s, 2H, N-CH_2), 3.20 (s, 3H, CH_3), 2.68 (d, J = 12.1 Hz, 2H), 1.99 (s, 6H), 1.84 – 1.17 (m, 7H). ^{13}C NMR (100 MHz, DMSO-d_6) δ 167.9, 165.2, 161.5, 160.3, 158.5,

152.1, 150.6, 150.4, 149.5, 143.4, 143.1, 142.0, 131.7, 129.4, 128.6, 128.2, 126.0, 122.1, 120.0, 119.4, 107.1, 96.4, 62.0, 52.5, 48.6, 31.7, 24.7, 16.5. ESI-MS: m/z 610.7 $[M + H]^+$, 632.4 $[M + Na]^+$. $C_{33}H_{35}N_7O_3S$ (609.25). HPLC purity: 99.05%.

(*E*)-3-(3,5-dimethyl-4-((5-(2-methylpyridin-4-yl)-2-((1-(4-(methylsulfonyl)benzyl) piperidin-4-yl)amino)pyrimidin-4-yl)oxy)phenyl)acrylonitrile (24b)

24b was synthesized from **21b** (643 mg, 1.0 mmol) and (2-methylpyridin-4-yl)boronic acid (164 mg, 1.2 mmol). White solid, 58% yield, mp: 125-127°C. ^{1}H NMR (400 MHz, DMSO-d_6) δ 8.47 (dd, J = 14.3, 7.6 Hz, 2H), 7.88 (d, J = 7.8 Hz, 2H), 7.57 (dt, J = 25.1, 13.8 Hz, 5H), 7.46 (s, 2H), 6.89 (s, 1H, NH), 6.41 (d, J = 16.7 Hz, 1H, =CHCN), 3.54 – 3.42 (m, 2H, N-CH_2), 3.20 (s, 3H, SO_2CH_3), 2.84 – 3.76 (m, 2H), 2.48 (s, 3H, CH_3), 2.06 (s, 6H), 2.00 – 1.19 (m, 7H). ^{13}C NMR (100 MHz, DMSO-d_6) δ 170.7, 167.2, 165.3, 161.5, 158.5, 150.8, 149.5, 145.5, 139.8, 131.5, 129.8, 127.4, 120.4, 105.9, 96.7, 61.9, 52.8, 44.0, 31.2, 24.7, 16.8. ESI-MS: m/z 609.7 $[M + H]^+$, 626.5 $[M + NH_4]^+$. $C_{34}H_{36}N_6O_3S$ (608.26). HPLC purity: 99.36%.

(*E*)-4-((4-((4-(4-(2-cyanovinyl)-2,6-dimethylphenoxy)-5-(2-methylpyridin-4-yl) pyrimidin-2-yl)amino)piperidin-1-yl)methyl)benzamide (24c)

24c was synthesized from **21c** (608 mg, 1.0 mmol) and (2-methylpyridin-4-yl)boronic acid (164 mg, 1.2 mmol). White solid, 61% yield, mp: 127-129°C. ^{1}H NMR (400 MHz, DMSO-d_6) δ 8.40 (dd, J = 13.8, 7.4 Hz, 2H), 7.84 (s, 1H), 7.75 (d, J = 7.7 Hz, 2H), 7.50 – 7.44 (m, 3H), 7.39 (s, 2H), 7.32 – 7.14 (m, 3H), 6.89 (s, 1H, NH), 6.42 – 6.27 (m, 1H, =CHCN), 3.40 (s, 2H, N-CH_2), 3.20 (s, 3H, CH_3), 2.72 (d, J = 26.0 Hz, 2H), 1.96 (s, 6H), 1.91 – 1.12 (m, 7H). ^{13}C NMR (100 MHz, DMSO-d_6) δ 168.2, 165.3, 158.4, 150.5, 149.5, 142.5, 133.4, 131.6, 128.8, 127.8, 121.6, 119.4, 114.4, 96.6, 62.3, 57.6, 52.8, 31.7, 24.7, 16.8. ESI-MS: m/z 574.5 $[M + H]^+$, 596.3 $[M + Na]^+$. $C_{34}H_{35}N_7O_2$ (573.29). HPLC purity: 98.77%.

(*E*)-4-((4-((4-(4-(2-cyanovinyl)-2,6-dimethylphenoxy)-5-(2-fluoropyridin-4-yl)pyrimidin-2-yl)amino)piperidin-1-yl)methyl)benzenesulfonamide (25a)

25a was synthesized from **21a** (644 mg, 1.0 mmol) and (2-fluoropyridin-4-yl)boronic acid (169 mg, 1.2 mmol). White solid, 59% yield, mp: 222-224°C. ^{1}H NMR (400 MHz, DMSO-d_6) δ 8.56 (d, J = 12.0 Hz, 1H), 8.19 (d, J = 5.3 Hz, 1H), 7.71 – 7.62 (m, 5H), 7.50 – 7.37 (m, 4H), 7.25 (d, J = 10.6 Hz, 2H), 6.89 (s, 1H, NH), 6.36 (d, J = 15.6 Hz, 1H, =CHCN), 3.58 – 3.28 (m, 2H, N-CH_2), 2.69 (s, 2H), 2.00 (s, 6H), 1.90 – 1.20 (m, 7H). ^{13}C NMR (100 MHz, DMSO-d_6) δ 165.1, 160.7, 156.0, 153.1, 151.9, 150.6, 150.4, 148.1, 143.4, 131.7 (d, J_{CF} = 13 Hz), 129.3, 128.6, 128.2 (d, J_{CF} = 8 Hz), 126.1, 121.3, 119.3, 104.6, 96.9, 52.5, 45.8, 29.0, 16.8. ESI-MS: m/z 614.4 $[M + H]^+$, 636.5 $[M + Na]^+$. $C_{32}H_{32}FN_7O_3S$ (613.23). HPLC purity: 98.95%.

(*E*)-3-(4-((5-(2-fluoropyridin-4-yl)-2-((1-(4-(methylsulfonyl)benzyl)piperidin-4-yl) amino)pyrimidin-4-yl)oxy)-3,5-dimethylphenyl)acrylonitrile (25b)

25b was synthesized from **21b** (643 mg, 1.0 mmol) and (2-fluoropyridin-4-yl)boronic acid (169 mg, 1.2 mmol). White solid, 57% yield, mp: 147-149°C. ^{1}H NMR (400 MHz, DMSO-d_6) δ 8.63 (d, J = 11.2 Hz, 1H), 8.31 – 8.22 (m, 1H), 7.88 (d, J = 7.9 Hz, 2H), 7.81 – 7.60

(m, 2H), 7.60 – 7.50 (m, 3H), 7.46 (d, J = 10.6 Hz, 2H), 6.70 (s, 1H, NH), 6.53 – 6.35 (m, 1H, =CHCN), 3.49 – 3.48 (m, 2H), 3.21 (s, 3H, SO_2CH_3), 2.94 – 2.55 (m, 2H), 2.07 (s, 6H), 1.95 – 1.05 (m, 7H). ^{13}C NMR (100 MHz, DMSO-d_6) δ 165.3, 160.7, 147.9, 145.4, 139.8, 132.5, 132.0 (d, J_{CF} = 10 Hz), 131.7, 131.6, 129.8 (d, J_{CF} = 9 Hz), 129.2 (d, J_{CF} = 11 Hz), 128.6, 128.2, 127.3, 120.8, 119.3, 107.4, 90.5, 52.7, 44.0, 31.7, 16.8. ESI-MS: m/z 613.4 [M + H]$^+$, 635.3 [M + Na]$^+$. $C_{33}H_{33}FN_6O_3S$ (612.23). HPLC purity: 98.56%.

(*E*)-4-((4-((4-(4-(2-cyanovinyl)-2,6-dimethylphenoxy)-5-(2-fluoropyridin-4-yl) pyrimidin-2-yl)amino)piperidin-1-yl)methyl)benzamide (25c)

25c was synthesized from **21c** (608 mg, 1.0 mmol) and (2-fluoropyridin-4-yl)boronic acid (169 mg, 1.2 mmol). White solid, 49% yield, mp: 173-175°C. ^{1}H NMR (400 MHz, DMSO-d_6) δ 8.63 (d, J = 11.1 Hz, 1H), 8.26 (d, J = 5.3 Hz, 1H), 8.04 – 7.54 (m, 5H), 7.46 (d, J = 10.6 Hz, 4H), 7.33 (d, J = 8.1 Hz, 2H), 6.70 (s, 1H, NH), 6.43 (d, J = 16.9 Hz, 1H, =CHCN), 3.41 (s, 2H, N-CH_2), 2.74 (s, 2H), 2.07 (s, 6H), 1.99 – 1.28 (m, 7H). ^{13}C NMR (100 MHz, DMSO-d_6) δ 168.2, 165.3, 158.8, 157.6, 152.7, 150.5, 148.1, 142.6, 133.2, 131.6, 127.9, 119.3, 115.0, 110.7, 107.0, 96.8, 52.5, 48.9, 29.0, 18.9, 16.5. ESI-MS: m/z 578.5 [M + H]$^+$, 600.5 [M + Na]$^+$. $C_{33}H_{32}FN_7O_2$ (577.26). HPLC purity: 97.77%.

(*E*)-4-((4-((5-(2-chloropyridin-4-yl)-4-(4-(2-cyanovinyl)-2,6-dimethylphenoxy) pyrimidin-2-yl)amino)piperidin-1-yl)methyl)benzenesulfonamide (26a)

26a was synthesized from **21a** (644 mg, 1.0 mmol) and (2-chloropyridin-4-yl)boronic acid (188 mg, 1.2 mmol). White solid, 68% yield, mp: 133-135°C. ^{1}H NMR (400 MHz, DMSO-d_6) δ 8.53 (d, J = 14.2 Hz, 1H), 8.35 (d, J = 5.2 Hz, 1H), 7.75 – 7.70 (m, 4H), 7.55 (d, J = 16.7 Hz, 1H, ArCH=), 7.38 (d, J = 10.7 Hz, 4H), 7.24 (d, J = 6.8 Hz, 2H), 6.90 (s, 1H, NH), 6.35 (d, J = 16.6, 1H, =CHCN), 3.43 (s, 2H, N-CH_2), 2.86 – 2.58 (m, 2H), 1.99 (s, 6H), 1.90 – 0.98 (m, 7H). ^{13}C NMR (100 MHz, DMSO-d_6) δ 168.4, 150.6, 145.7, 143.3, 143.1, 131.7, 129.4, 128.6, 128.2, 126.0, 122.0, 119.4, 105.7, 96.8, 62.0, 52.5, 49.7, 31.2, 23.8, 16.5. ESI-MS: m/z 630.7 [M + H]$^+$, 652.2 [M + Na]$^+$. $C_{32}H_{32}ClN_7O_3S$ (629.20). HPLC purity: 98.11%.

(*E*)-3-(4-((5-(2-chloropyridin-4-yl)-2-((1-(4-(methylsulfonyl)benzyl)piperidin-4-yl)amino)pyrimidin-4-yl)oxy)-3,5-dimethylphenyl)acrylonitrile (26b)

26b was synthesized from **21b** (643 mg, 1.0 mmol) and (2-chloropyridin-4-yl)boronic acid (188 mg, 1.2 mmol). White solid, 51% yield, mp: 130-132°C. ^{1}H NMR (400 MHz, DMSO-d_6) δ 8.60 (d, J = 14.0 Hz, 1H), 8.42 (d, J = 5.2 Hz, 1H), 7.87 – 7.81 (m, 3H), 7.76 (d, J = 8.9 Hz, 2H), 7.67 – 7.49 (m, 2H), 7.45 (d, J = 8.9 Hz, 2H), 6.89 (s, 1H, NH), 6.50 – 6.32 (m, 1H, =CHCN), 3.48 (s, 2H, N-CH_2), 3.20 (s, 3H, SO_2CH_3), 2.84 – 2.56 (m, 2H), 2.06 (s, 6H), 1.98 – 1.17 (m, 7H). ^{13}C NMR (100 MHz, DMSO-d_6) δ 168.7, 165.3, 161.8, 160.4, 153.6, 151.2, 150.6, 150.3, 145.5, 139.8, 131.7, 129.8, 128.6, 128.2, 127.4, 122.3, 119.4, 112.6, 96.5, 61.9, 52.6, 44.0, 31.7, 29.0, 16.6. ESI-MS: m/z 629.6 [M + H]$^+$, 646.2 [M + NH_4]$^+$. $C_{33}H_{33}ClN_6O_3S$ (628.20). HPLC purity: 97.28%.

(*E*)-4-((4-((5-(2-chloropyridin-4-yl)-4-(4-(2-cyanovinyl)-2,6-dimethylphenoxy) pyrimidin-2-yl)amino)piperidin-1-yl)methyl)benzamide (26c)

26c was synthesized from **21c** (608 mg, 1.0 mmol) and (2-chloropyridin-4-yl)boronic acid (188 mg, 1.2 mmol). White solid, 57% yield, mp: 123-127°C. ^{1}H NMR (400 MHz, DMSO-d_6) δ 8.53 (d, J = 13.4 Hz, 1H), 8.35 (d, J = 5.2 Hz, 1H), 7.84 (s, 1H), 7.75 (d, J = 7.9 Hz, 3H), 7.68 (d, J = 9.8 Hz, 1H), 7.54 (t, J = 17.3 Hz, 1H, ArCH=), 7.39 (s, 2H), 7.25 (dd, J = 14.0, 7.3 Hz, 3H), 6.89 (s, 1H, NH), 6.35 (d, J = 16.7 Hz, 1H, =CHCN), 3.40 (s, 2H, N-CH_2), 2.87 – 2.63 (m, 2H), 1.99 (s, 6H), 1.93 – 1.12 (m, 7H). ^{13}C NMR (100 MHz, DMSO-d_6) δ 168.2, 164.3, 161.7, 160.7, 152.4, 150.3, 145.5, 142.5, 133.4, 131.7, 128.9, 127.9, 122.4, 121.8, 119.3, 96.8, 62.3, 52.5, 31.2, 23.7, 16.5. ESI-MS: m/z 594.3 $[M + H]^+$, 616.5 $[M + Na]^+$. $C_{33}H_{32}ClN_7O_2$ (593.23). HPLC purity: 99.15%.

(*E*)-4-((4-((5-(2-bromopyridin-4-yl)-4-(4-(2-cyanovinyl)-2,6-dimethylphenoxy) pyrimidin-2-yl)amino)piperidin-1-yl)methyl)benzenesulfonamide (27a)

27a was synthesized from **21a** (644 mg, 1.0 mmol) and (2-bromopyridin-4-yl)boronic acid (241 mg, 1.2 mmol). White solid, 64% yield, mp: 183-185°C. ^{1}H NMR (400 MHz, DMSO-d_6) δ 8.56 (d, J = 11.4 Hz, 1H), 8.20 (d, J = 5.3 Hz, 1H), 7.71 – 7.62 (m, 3H), 7.57 – 7.55 (m, 2H), 7.50 – 7.37 (m, 4H), 7.25 (d, J = 8.6 Hz, 2H), 6.89 (s, 1H, NH), 6.36 – 6.35 (m, 1H, =CHCN), 3.58 – 3.28 (m, 2H, N-CH_2), 2.69 (s, 2H), 2.00 (s, 6H), 1.90 – 1.20 (m, 7H). ^{13}C NMR (100 MHz, DMSO-d_6) δ 170.2, 165.8, 161.5, 156.9, 153.9, 151.3, 144.5, 143.4, 137.7, 131.7, 129.4, 126.9, 126.2, 122.2, 107.9, 90.7, 52.6, 50.6, 45.8, 29.0, 16.5. ESI-MS: m/z 674.5 $[M + H]^+$, 696.4 $[M + Na]^+$. $C_{32}H_{32}BrN_7O_3S$ (673.15). HPLC purity: 98.66%.

(*E*)-3-(4-((5-(2-bromopyridin-4-yl)-2-((1-(4-(methylsulfonyl)benzyl)piperidin-4-yl)amino)pyrimidin-4-yl)oxy)-3,5-dimethylphenyl)acrylonitrile (27b)

27b was synthesized from **21b** (643 mg, 1.0 mmol) and (2-bromopyridin-4-yl)boronic acid (241 mg, 1.2 mmol). White solid, 57% yield, mp: 157-159°C. ^{1}H NMR (400 MHz, DMSO-d_6) δ 8.41 (s, 1H), 7.87 (d, J = 7.1 Hz, 2H), 7.65 – 7.49 (m, 4H), 7.45 (s, 2H), 7.28 – 7.14 (m, 2H), 6.70 (s, 1H, NH), 6.40 (d, J = 16.7 Hz, 1H, =CHCN), 3.56 – 3.52 (m, 2H), 3.19 (s, 3H, SO_2CH_3), 2.74 (s, 2H), 2.05 (s, 6H), 1.98 – 1.39 (m, 7H). ^{13}C NMR (100 MHz, DMSO-d_6) δ 166.2, 161.4, 150.5, 145.4, 145.4, 139.8, 131.7, 131.6, 131.4, 131.1, 129.8, 129.7, 128.6, 127.3, 120.7, 119.3, 101.2, 96.2, 61.9, 52.7, 50.6, 29.0, 16.5. ESI-MS: m/z 673.5 $[M + H]^+$, 695.2 $[M + Na]^+$. $C_{33}H_{33}BrN_6O_3S$ (672.15). HPLC purity: 99.54%.

(*E*)-4-((4-((5-(2-bromopyridin-4-yl)-4-(4-(2-cyanovinyl)-2,6-dimethylphenoxy) pyrimidin-2-yl)amino)piperidin-1-yl)methyl)benzamide (27c)

27c was synthesized from **21c** (608 mg, 1.0 mmol) and (2-bromopyridin-4-yl)boronic acid (241 mg, 1.2 mmol). White solid, 55% yield, mp: 178-180°C. ^{1}H NMR (400 MHz, DMSO-d_6) δ 8.41 – 8.40 (m, 1H), 7.95 (s, 2H), 7.83 (d, J = 7.1 Hz, 2H), 7.69 – 7.54 (m, 3H), 7.46 (s, 2H), 7.30 – 7.28 (m, 3H), 6.71 (s, 1H, NH), 6.43 (d, J = 16.7 Hz, 1H, =CHCN), 3.42 (s, 2H, N-CH_2), 2.75 (s, 2H), 2.10 (s, 6H), 1.97 – 1.12 (m, 7H). ^{13}C NMR (100 MHz, DMSO-d_6) δ 168.2, 165.8, 161.3, 157.1, 151.4, 150.5, 146.1, 144.2, 142.6, 133.7, 131.7, 131.4, 131.0, 128.9, 127.9, 122.9, 119.3, 110.0, 100.4, 96.5, 52.7, 50.6, 29.0, 16.4. ESI-MS: m/z 638.4 $[M + H]^+$, 655.4 $[M + NH_4]^+$. $C_{33}H_{32}BrN_7O_2$ (637.18). HPLC purity: 99.18%.

(*E*)-4-((4-((4-(4-(2-cyanovinyl)-2,6-dimethylphenoxy)-5-(pyridin-3-yl)pyrimidin-2-yl)amino)piperidin-1-yl)methyl)benzenesulfonamide (28a)

28a was synthesized from **21a** (644 mg, 1.0 mmol) and pyridin-3-ylboronic acid (147 mg, 1.2 mmol). White solid, 62% yield, mp: 148-150°C. ^{1}H NMR (400 MHz, DMSO-d_6) δ 8.78 (d, J = 18.1 Hz, 1H), 8.45 (dd, J = 4.8, 1.6 Hz, 1H), 8.34 (d, J = 3.3 Hz, 1H), 7.98 (s, 1H), 7.71 (d, J = 7.9 Hz, 2H), 7.51– 7.39 (m, 6H), 7.31 – 7.21 (m, 2H), 7.11 (d, J = 8.2 Hz, 1H), 6.34 (d, J = 17.5 Hz, 1H, =CHCN), 3.42 (s, 2H), 2.88 – 2.52 (m, 2H), 1.99 (s, 6H), 1.82 – 1.12 (m, 7H). ^{13}C NMR (100 MHz, DMSO) δ 165.2, 161.4, 160.0, 159.5, 149.2, 148.2, 143.4, 143.1, 136.2, 131.6, 129.4, 128.1, 126.0, 124.0, 119.4, 113.7, 96.6, 91.2, 61.9, 52.8, 31.2, 29.0, 16.6. ESI-MS: m/z 596.3 $[M + H]^+$, 618.5 $[M + Na]^+$. $C_{32}H_{33}N_7O_3S$ (595.24). HPLC purity: 98.99%.

(*E*)-3-(3,5-dimethyl-4-((2-((1-(4-(methylsulfonyl)benzyl)piperidin-4-yl)amino)-5-(pyridin-3-yl)pyrimidin-4-yl)oxy)phenyl)acrylonitrile (28b)

28b was synthesized from **21b** (643 mg, 1.0 mmol) and pyridin-3-ylboronic acid (147 mg, 1.2 mmol). White solid, 39% yield, mp: 193-195°C. ^{1}H NMR (400 MHz, DMSO-d_6) δ 8.78 (d, J = 17.4 Hz, 1H), 8.45 (dd, J = 4.7, 1.6 Hz, 1H), 8.34 (d, J = 3.3 Hz, 1H), 7.99 (d, J = 13.9 Hz, 1H), 7.81 (d, J = 7.9 Hz, 2H), 7.59 – 7.35 (m, 7H), 6.34 (d, J = 16.7 Hz, 1H, =CHCN), 3.41 (s, 2H), 3.14 (s, 3H, SO_2CH_3), 2.84 – 2.49 (m, 2H), 1.99 (s, 6H), 1.78 – 1.12 (m, 7H). ^{13}C NMR (100 MHz, DMSO) δ 165.2, 161.4, 159.6, 154.7, 152.1, 150.6, 149.3, 148.2, 145.5, 139.8, 136.1, 135.8, 131.6, 131.5, 129.7, 127.4, 124.0, 119.4, 106.5, 96.7, 61.9, 52.6, 44.0, 31.3, 16.6. ESI-MS: m/z 595.5 $[M + H]^+$, 617.4 $[M + Na]^+$. $C_{33}H_{34}N_6O_3S$ (594.24). HPLC purity: 98.41%.

(*E*)-4-((4-((4-(4-(2-cyanovinyl)-2,6-dimethylphenoxy)-5-(pyridin-3-yl)pyrimidin-2-yl)amino)piperidin-1-yl)methyl)benzamide (28c)

28c was synthesized from **21c** (608 mg, 1.0 mmol) and pyridin-3-ylboronic acid (147 mg, 1.2 mmol). White solid, 37% yield, mp: 234-236°C. ^{1}H NMR (400 MHz, DMSO-d_6) δ 8.78 (d, J = 17.3 Hz, 1H), 8.50 – 8.41 (m, 1H), 8.34 (d, J = 3.0 Hz, 1H), 7.99 (d, J = 12.6 Hz, 1H), 7.86 (s, 1H), 7.76 (d, J = 7.8 Hz, 2H), 7.55 (d, J = 17.7 Hz, 1H), 7.46 – 7.35 (m, 3H), 7.29 – 7.25 (m, 3H), 7.10 (d, J = 7.1 Hz, 1H), 6.34 (d, J = 16.7 Hz, 1H, =CHCN), 3.41 (s, 2H), 2.84 – 2.60 (m, 2H), 1.99 (s, 6H), 1.87 – 1.12 (m, 7H). ^{13}C NMR (100 MHz, DMSO-d_6) δ 168.2, 165.2, 161.4, 159.5, 150.5, 149.1, 148.2, 136.2, 133.4, 131.6, 131.5, 128.8, 127.8, 124.0, 119.4, 96.6, 90.7, 62.2, 52.7, 39.6, 16.7. ESI-MS: m/z 560.2 $[M + H]^+$, 577.5 $[M + NH_4]^+$. $C_{33}H_{33}N_7O_2$ (559.27). HPLC purity: 97.55%.

(*E*)-4-((4-((5-(6-aminopyridin-3-yl)-4-(4-(2-cyanovinyl)-2,6-dimethylphenoxy) pyrimidin-2-yl)amino)piperidin-1-yl)methyl)benzenesulfonamide (29a)

29a was synthesized from **21a** (644 mg, 1.0 mmol) and (6-aminopyridin-3-yl)boronic acid (165 mg, 1.2 mmol). White solid, 51% yield, mp: 146-148°C. ^{1}H NMR (400 MHz, DMSO-d_6) δ 8.16 (d, J = 3.4 Hz, 1H), 8.06 (s, 1H), 7.71 (dd, J = 8.3, 2.7 Hz, 2H), 7.56 – 7.52 (m, 3H), 7.38 (d, J = 6.5 Hz, 4H), 7.25 (s, 2H), 6.45 (d, J = 8.6 Hz, 1H), 6.33 (d, J = 16.7 Hz, 1H, =CHCN), 5.93 (s, 2H), 3.40 (s, 2H, N-CH_2), 2.87 – 2.74 (m, 2H), 1.97 (s, 6H), 1.82 – 1.02 (m, 7H). ^{13}C NMR (100 MHz, DMSO-d_6) δ 165.2, 160.7, 159.1, 152.4, 150.6,

147.3, 143.1, 137.6, 131.6, 131.3, 129.4, 128.4, 126.0, 119.4, 118.1, 108.0, 96.4, 62.0, 52.7, 31.5, 16.7. ESI-MS: m/z 611.3 $[M + H]^+$, 633.7 $[M + Na]^+$. $C_{32}H_{34}N_8O_3S$ (610.25). HPLC purity: 98.63%.

(*E*)-3-(4-((5-(6-aminopyridin-3-yl)-2-((1-(4-(methylsulfonyl)benzyl)piperidin-4-yl)amino)pyrimidin-4-yl)oxy)-3,5-dimethylphenyl)acrylonitrile (29b)

29b was synthesized from **21b** (643 mg, 1.0 mmol) and (6-aminopyridin-3-yl)boronic acid (165 mg, 1.2 mmol). White solid, 40% yield, mp: 209-211°C. ^{1}H NMR (400 MHz, DMSO-d_6) δ 8.23 (d, J = 3.4 Hz, 1H), 8.14 (s, 1H), 7.88 (d, J = 7.9 Hz, 2H), 7.62 – 7.57 (m, 3H), 7.53 (d, J = 7.7 Hz, 2H), 7.44 (s, 2H), 6.52 (d, J = 8.6 Hz, 1H), 6.40 (d, J = 16.7 Hz, 1H, =CHCN), 6.00 (s, 2H), 3.41 (s, 2H, N-CH_2), 3.20 (s, 3H, SO_2CH_3), 2.80 – 2.67 (m, 2H), 2.06 (s, 6H), 1.87 – 1.21 (m, 7H). ^{13}C NMR (100 MHz, DMSO-d_6) δ 165.2, 160.7, 159.1, 148.6, 147.3, 145.5, 139.8, 137.6, 131.6, 131.3, 129.8, 129.7, 127.4, 119.4, 118.1, 108.0, 61.9, 52.7, 44.0, 31.6, 16.7. ESI-MS: m/z 611.2 $[M + H]^+$. $C_{33}H_{35}N_7O_3S$ (609.25). HPLC purity: 98.39%.

(*E*)-4-((4-((5-(6-aminopyridin-3-yl)-4-(4-(2-cyanovinyl)-2,6-dimethylphenoxy) pyrimidin-2-yl)amino)piperidin-1-yl)methyl)benzamide (29c)

29c was synthesized from **21c** (608 mg, 1.0 mmol) and (6-aminopyridin-3-yl)boronic acid (165 mg, 1.2 mmol). White solid, 47% yield, mp: 182-184°C. ^{1}H NMR (400 MHz, DMSO-d_6) δ 8.23 (d, J = 3.8 Hz, 1H), 8.13 (s, 1H), 7.96 (s, 1H), 7.84 (d, J = 7.8 Hz, 2H), 7.61 (d, J = 14.4 Hz, 3H), 7.44 (s, 2H), 7.40 – 7.27 (m, 4H), 6.53 (d, J = 8.6 Hz, 1H), 6.41 (d, J = 16.7 Hz, 1H, =CHCN), 6.02 (s, 2H), 3.41 (s, 2H, N-CH_2), 2.81 – 2.58 (m, 2H), 2.05 (s, 6H), 1.82 – 1.10 (m, 7H). ^{13}C NMR (100 MHz, DMSO) δ 172.4, 168.2, 165.1, 160.7, 159.1, 150.5, 147.3, 144.4, 137.7, 131.6, 130.1, 129.3, 127.9, 119.4, 118.0, 108.0, 96.5, 90.0, 53.8, 33.1, 29.5, 16.7. ESI-MS: m/z 575.3 $[M + H]^+$, 597.1 $[M + Na]^+$. $C_{33}H_{34}N_8O_2$ (574.28). HPLC purity: 98.06%.

(*E*)-4-((4-((4-(4-(2-cyanovinyl)-2,6-dimethylphenoxy)-5-(6-fluoropyridin-3-yl)pyrimidin-2-yl)amino)piperidin-1-yl)methyl)benzenesulfonamide (30a)

30a was synthesized from **21a** (644 mg, 1.0 mmol) and (6-fluoropyridin-3-yl)boronic acid (169 mg, 1.2 mmol). White solid, 71% yield, mp: 118-120°C. ^{1}H NMR (400 MHz, DMSO-d_6) δ 8.41 (d, J = 18.3 Hz, 1H), 8.33 (s, 1H), 8.18 (s, 1H), 7.71 (dd, J = 7.1, 3.6 Hz, 2H), 7.62 – 7.48 (m, 1H), 7.39 (d, J = 11.2 Hz, 4H), 7.28 – 7.17 (m, 4H), 6.34 (d, J = 16.5 Hz, 1H, =CHCN), 3.55 – 3.52 (m, 2H), 2.81 – 2.50 (m, 2H), 1.99 (s, 6H), 1.75 – 1.15 (m, 7H). ^{13}C NMR (100 MHz, DMSO) δ 165.1, 161.5, 159.5, 152.5, 150.6, 148.5, 146.9 (J_{CF} = 20 Hz), 143.4 (J_{CF} = 23 Hz), 142.1, 131.6, 131.5, 128.7, 126.9, 126.0, 119.4, 110.0, 109.6, 104.4, 96.6, 62.0, 52.8, 31.7, 29.0, 16.8. ESI-MS: m/z 614.2 $[M + H]^+$, 636.4 $[M + Na]^+$. $C_{32}H_{32}FN_7O_3S$ (613.23). HPLC purity: 99.23%.

(*E*)-3-(4-((5-(6-fluoropyridin-3-yl)-2-((1-(4-(methylsulfonyl)benzyl)piperidin-4-yl)amino)pyrimidin-4-yl)oxy)-3,5-dimethylphenyl)acrylonitrile (30b)

30b was synthesized from **21b** (643 mg, 1.0 mmol) and (6-fluoropyridin-3-yl)boronic acid (169 mg, 1.2 mmol). White solid, 61% yield, mp: 115-117°C. ^{1}H NMR (400 MHz, DMSO-

d_6) δ 8.42 (d, J = 17.7 Hz, 1H), 8.33 (s, 1H), 8.17 (d, J = 8.5 Hz, 1H), 7.81 (d, J = 8.0 Hz, 2H), 7.57 – 7.41 (m, 4H), 7.38 (s, 2H), 7.20 (dd, J = 8.6, 2.9 Hz, 1H), 6.34 (d, J = 16.7 Hz, 1H, =CHCN), 3.46 – 3.42 (m, 2H), 3.14 (s, 3H, SO_2CH_3), 2.79 – 2.49 (m, 2H), 1.99 (s, 6H), 1.76 – 1.06 (m, 7H). ^{13}C NMR (100 MHz, DMSO) δ 165.1, 161.5, 161.2, 160.0, 150.6, 146.9 (J_{CF} = 20 Hz), 145.5, 142.4, 139.8, 131.6 (J_{CF} = 10 Hz), 129.8, 128.7, 128.1, 127.4, 124.5, 119.4, 109.9, 96.6, 61.9, 52.6, 44.0, 31.7, 16.6. ESI-MS: m/z 613.5 $[M + H]^+$, 635.3 $[M + Na]^+$. $C_{33}H_{33}FN_6O_3S$ (612.23). HPLC purity: 97.95%.

(*E*)-4-((4-((4-(4-(2-cyanovinyl)-2,6-dimethylphenoxy)-5-(6-fluoropyridin-3-yl)pyrimidin-2-yl)amino)piperidin-1-yl)methyl)benzamide (30c)

30c was synthesized from **21c** (608 mg, 1.0 mmol) and (6-fluoropyridin-3-yl)boronic acid (169 mg, 1.2 mmol). White solid, 65% yield, mp: 113-115°C. ^{1}H NMR (400 MHz, DMSO-d_6) δ 8.41 (d, J = 17.7 Hz, 1H), 8.33 (s, 1H), 8.18 (s, 1H), 7.86 (s, 1H), 7.76 (d, J = 7.7 Hz, 2H), 7.60 – 7.47 (m, 1H), 7.38 (s, 2H), 7.31 – 7.09 (m, 5H), 6.34 (d, J = 16.7 Hz, 1H, =CHCN), 3.54 – 3.53 (m, 2H), 2.77 – 2.73 (m, 2H), 1.99 (s, 6H), 1.83 – 1.10 (m, 7H). ^{13}C NMR (100 MHz, DMSO) δ 168.2, 165.1, 161.2, 159.4, 155.8, 150.4, 146.7, 142.4, 133.4, 131.6 (J_{CF} = 10 Hz), 128.8, 127.8, 119.4, 109.9, 109.6, 96.6, 62.3, 52.8, 31.5, 29.0, 16.8. ESI-MS: m/z 578.6 $[M + H]^+$, 600.4 $[M + Na]^+$. $C_{33}H_{32}FN_7O_2$ (577.26). HPLC purity: 98.52%.

Supplementary Material

Refer to Web version on PubMed Central for supplementary material.

ACKNOWLEDGMENTS

We gratefully acknowledge financial support from the National Natural Science Foundation of China (NSFC Nos. 81973181, 81903453), Shandong Provincial Key research and development project (Nos. 2019JZZY021011), Shandong Provincial Natural Science Foundation (ZR2019BH011, ZR2020YQ61, ZR2020JQ31), Foreign cultural and educational experts Project (GXL20200015001), Young Scholars Program of Shandong University (YSPSDU No. 2016WLJH32), National Science and Technology Major Projects for "Major New Drugs Innovation and Development" (2019ZX09301126), the Taishan Scholar Program at Shandong Province, KU Leuven (GOA 10/014), and NIH grant R01 AI027690 (to E.A.). The technical assistance of Mr. Kris Uyttersprot and Mrs. Kristien Erven, for the HIV experiments is gratefully acknowledged.

ABBREVIATIONS USED

AIDS	acquired immune deficiency syndrome
cART	combination antiretroviral therapy
CC_{50}	50% cytotoxicity concentration
C_{max}	maximum concentration
DAPY	diarylpyrimidine
DLV	delavirdine
DOR	doravirine

EFV	efavirenz
ETV	etravirine
EC_{50}	the effective concentration causing 50% inhibition of viral cytopathogenicity
FDA	U.S. Food and Drug Administration
HIV	human immunodeficiency virus
hERG	the human ether-à-go-go related gene
NNIBP	NNRTI-binding pocket
NNRTI	non-nucleoside RT inhibitor
NRTI	nucleoside RT inhibitor
NVP	nevirapine
RF	fold-resistance
RPV	rilpivirine
RT	reverse transcriptase
SAR	structure-activity relationship
SI	selectivity index
TLC	thin layer chromatography
TMS	tetramethylsilane
WT	wild type

References

1. https://www.who.int/hiv/data/en/.
2. Bec G; Meyer B; Gerard M-A; Steger J; Fauster K; Wolff P; Burnouf D; Micura R; Dumas P; Ennifar E Thermodynamics of HIV-1 reverse transcriptase in action elucidates the mechanism of action of non-nucleoside inhibitors. J. Am. Chem. Soc 2013, 135, 9743–9752. [PubMed: 23742167]
3. Namasivayam V; Vanangamudi M; Kramer VG; Kurup S; Zhan P; Liu X; Kongsted J; Byrareddy SN The journey of HIV-1 non-nucleoside reverse transcriptase inhibitors (NNRTIs) from lab to clinic. J. Med. Chem 2019, 62, 4851–4883. [PubMed: 30516990]
4. Zhuang C; Pannecouque C; De Clercq E; Chen F Development of non-nucleoside reverse transcriptase inhibitors (NNRTIs): our past twenty years. Acta Pharm. Sin. B 2020, 10, 961–978. [PubMed: 32642405]
5. Cilento ME , Kirby KA , & Sarafianos SG Avoiding drug resistance in hiv reverse transcriptase. Chem. Rev 2021. doi: 10.1021/acs.chemrev.0c00967.
6. Beyrer C; Pozniak A HIV drug resistance - an emerging threat to epidemic control. N. Engl. J. Med 2017, 377, 1605–1607. [PubMed: 29069566]

7. Battini L; Bollini M Challenges and approaches in the discovery of human immunodeficiency virus type-1 non-nucleoside reverse transcriptase inhibitors. Med. Res. Rev 2019, 39, 1235–1273. [PubMed: 30417402]
8. Kang D; Fang Z; Li Z; Huang B; Zhang H; Lu X; Xu H; Zhou Z; Ding X; Daelemans D; De Clercq E; Pannecouque C; Zhan P; Liu X Design, synthesis, and evaluation of thiophene[3,2-d]pyrimidine derivatives as HIV-1 non-nucleoside reverse transcriptase inhibitors with significantly improved drug resistance profiles. J. Med. Chem 2016, 59, 7991–8007. [PubMed: 27541578]
9. Kang D; Fang Z; Huang B; Lu X; Zhang H; Xu H; Huo Z; Zhou Z; Yu Z; Meng Q; Wu G; Ding X; Tian Y; Daelemans D; De Clercq E; Pannecouque C; Zhan P; Liu X Structure-based optimization of thiophene[3,2-d]pyrimidine derivatives as potent HIV-1 non-nucleoside reverse transcriptase inhibitors with improved potency against resistance-associated variants. J. Med. Chem 2017, 60, 4424–4443. [PubMed: 28481112]
10. Yang Y; Kang D; Nguyen LA; Smithline ZB; Pannecouque C; Zhan P; Liu X; Steitz TA Structural basis for potent and broad inhibition of HIV-1 RT by thiophene[3,2-d] pyrimidine non-nucleoside inhibitors. eLife 2018, 7, No. e36340 [PubMed: 30044217]
11. Kang D; Zhang H; Wang Z; Zhao T; Ginex T; Luque FJ; Yang Y; Wu G; Feng D; Wei F; Zhang J; De Clercq E; Pannecouque C; Chen CH; Lee K-H; Murugan NA; Steitz TA; Zhan P; Liu X Identification of dihydrofuro[3,4-d]pyrimidine derivatives as novel HIV-1 non-nucleoside reverse transcriptase inhibitors with promising antiviral activities and desirable physicochemical properties. J. Med. Chem 2019, 62, 1484–1501. [PubMed: 30624934]
12. Ishikawa M; Hashimoto Y Improvement in aqueous solubility in small molecule drug discovery programs by disruption of molecular planarity and symmetry. J. Med. Chem 2011, 54, 1539–1554. [PubMed: 21344906]
13. Kang D; Feng D; Sun Y; Fang Z; Wei F; De Clercq E; Pannecouque C; Liu X; Zhan P Structure-based bioisosterism yields HIV-1 NNRTIs with improved drug-resistance profiles and favorable pharmacokinetic properties. J. Med. Chem 2020, 63, 4837–4848. [PubMed: 32293182]
14. Kang D; Ruiz FX; Feng D; Pilch A; Zhao T; Wei F; Wang Z; Sun Y; Fang Z; De Clercq E; Pannecouque C; Arnold E; Liu X; Zhan P Discovery and characterization of fluorine-substituted diarylpyrimidine derivatives as Novel HIV-1 NNRTIs with highly improved resistance profiles and low activity for the hERG ion channel. J. Med. Chem 2020, 63, 1298–1312. [PubMed: 31935327]
15. Huang B; Chen W; Zhao T; Li Z; Jiang X; Ginex T; Vílchez D; Luque FJ; Kang D; Gao P; Zhang J; Tian Y; Daelemans D; De Clercq E; Pannecouque C; Zhan P; Liu X Exploiting the tolerant region I of the non-nucleoside reverse transcriptase inhibitor (NNRTI) binding pocket: discovery of potent diarylpyrimidine-typed HIV-1 NNRTIs against wild-type and E138K mutant virus with significantly improved water solubility and favorable safety profiles. J. Med. Chem 2019, 62, 2083–2098. [PubMed: 30721060]
16. Bauman JD; Das K; Ho WC; Baweja M; Himmel DM; Clark AD Jr.; Oren DA; Boyer PL; Hughes SH; Shatkin AJ; Arnold E Crystal engineering of HIV-1 reverse transcriptase for structure-based drug design. Nucleic Acids Res. 2008, 36, 5083–5092. [PubMed: 18676450]
17. Das K; Bauman JD; Clark AD Jr.; Frenkel YV; Lewi PJ; Shatkin AJ; Hughes SH; Arnold E High-resolution structures of HIV-1 reverse transcriptase/TMC278 complexes: strategic flexibility explains potency against resistance mutations. Proc.Natl. Acad. Sci. U. S. A 2008, 105, 1466–1471. [PubMed: 18230722]
18. Otwinowski Z; Minor W Processing of X-ray diffraction data collected in oscillation mode. Methods Enzymol. 1997, 276, 307–326.
19. Adams PD; Afonine PV; Bunkoczi G; Chen VB; Davis IW; Echols N; Headd JJ; Hung LW; Kapral GJ; Grosse-Kunstleve RW; McCoy AJ; Moriarty NW; Oeffner R; Read RJ; Richardson DC; Richardson JS; Terwilliger TC; Zwart PH PHENIX: a comprehensive python-based system for macromolecular structure solution. Acta Crystallogr., Sect. D: Biol. Crystallogr 2010, 66, 213–221. [PubMed: 20124702]
20. Emsley P; Cowtan K Coot: model-building tools for molecular graphics. Acta Crystallogr., Sect. D: Biol. Crystallogr 2004, 60, 2126–2132. [PubMed: 15572765]
21. Kang D; Feng D; Ginex T; Zou J; Wei F; Zhao T; Huang B; Sun Y; Desta S; De Clercq E; Pannecouque C; Zhan P; Liu X Exploring the hydrophobic channel of NNIBP leads to the

discovery of novel piperidine-substituted thiophene[3,2-d]pyrimidine derivatives as potent HIV-1 NNRTIs. Acta Pharm. Sin. B 2020, 10, 878–894. [PubMed: 32528834]

22. Kang D; Sun Y; Murugan NA; Feng D; Wei F; Li J; Jiang X; De Clercq E; Pannecouque C; Zhan P; Liu X Structure-activity relationship exploration of NNIBP tolerant region I leads to potent HIV-1 NNRTIs. ACS Infect. Dis 2020, 6, 2225–2234. [PubMed: 32619096]
23. Kuroda DG; Bauman JD; Challa JR; Patel D; Troxler T; Das K; Arnold E; Hochstrasser RM Snapshot of the equilibrium dynamics of a drug bound to HIV-1 reverse transcriptase. Nat. Chem 2013, 5, 174–181. [PubMed: 23422558]
24. Sarafianos SG; Marchand B; Das K; Himmel DM; Parniak MA; Hughes SH; Arnold E Structure and function of HIV-1 reverse transcriptase: molecular mechanisms of polymerization and inhibition. J. Mol. Biol 2009, 385, 693–713. [PubMed: 19022262]
25. Darby JF; Hopkins AP; Shimizu S; Roberts SM; Brannigan JA; Turkenburg JP; Thomas GH; Hubbard RE; Fischer M Water networks can determine the affinity of ligand binding to proteins. J. Am. Chem. Soc 2019, 141, 15818–15826. [PubMed: 31518131]
26. Schiebel J; Gaspari R; Wulsdorf T; Ngo K; Sohn C; Schrader TE; Cavalli A; Ostermann A; Heine A; Klebe G Intriguing role of water in protein-ligand binding studied by neutron crystallography on trypsin complexes. Nat. Commun 2018, 9, 3559. [PubMed: 30177695]
27. Rudling A; Orro A; Carlsson J Prediction of ordered water molecules in protein binding sites from molecular dynamics simulations: the impact of ligand binding on hydration networks. J. Chem. Inf. Model 2018, 58, 350–361. [PubMed: 29308882]
28. Huo Z; Zhang H; Kang D; Zhou Z; Wu G; Desta S; Zuo X; Wang Z; Jing L; Ding X; Daelemans D; De Clercq E; Pannecouque C; Zhan P; Liu X Discovery of novel diarylpyrimidine derivatives as potent HIV-1 NNRTIs targeting the "NNRTI adjacent" binding site. ACS Med. Chem. Lett 2018, 9, 334–338. [PubMed: 29670696]
29. Kang D; Huo Z; Wu G; Xu J; Zhan P; Liu X Novel fused pyrimidine and isoquinoline derivatives as potent HIV-1 NNRTIs: a patent evaluation of WO2016105532A1, WO2016105534A1 and WO2016105564A1. Expert Opin. Ther. Pat 2017, 27, 383–391. [PubMed: 28276283]

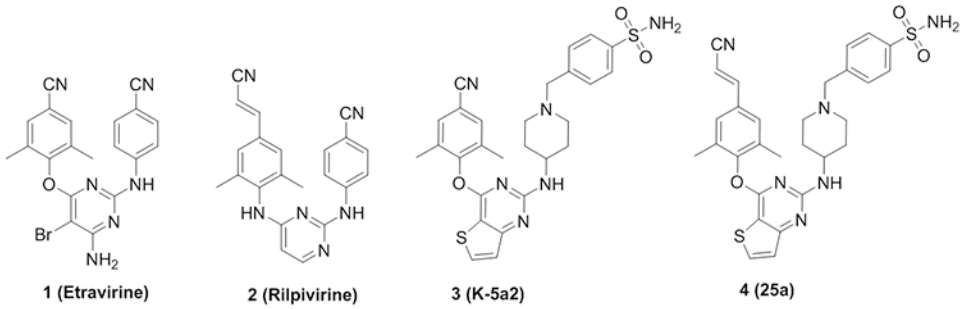

Figure 1.

The chemical structures of ETR, RPV, and the piperidine-substituted thiophene[3,2-d]pyrimidine compounds **K-5a2** and **25a**.

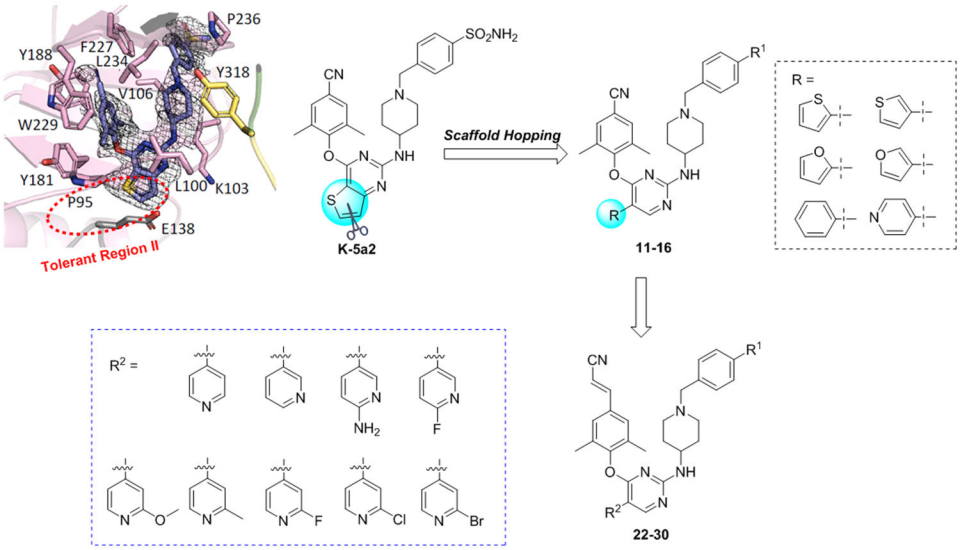

Figure 2.

Rational design of novel NNRTIs bearing the 2,4,5-trisubstituted pyrimidine scaffold utilizing scaffold hopping strategy (truncation of the fused ring).

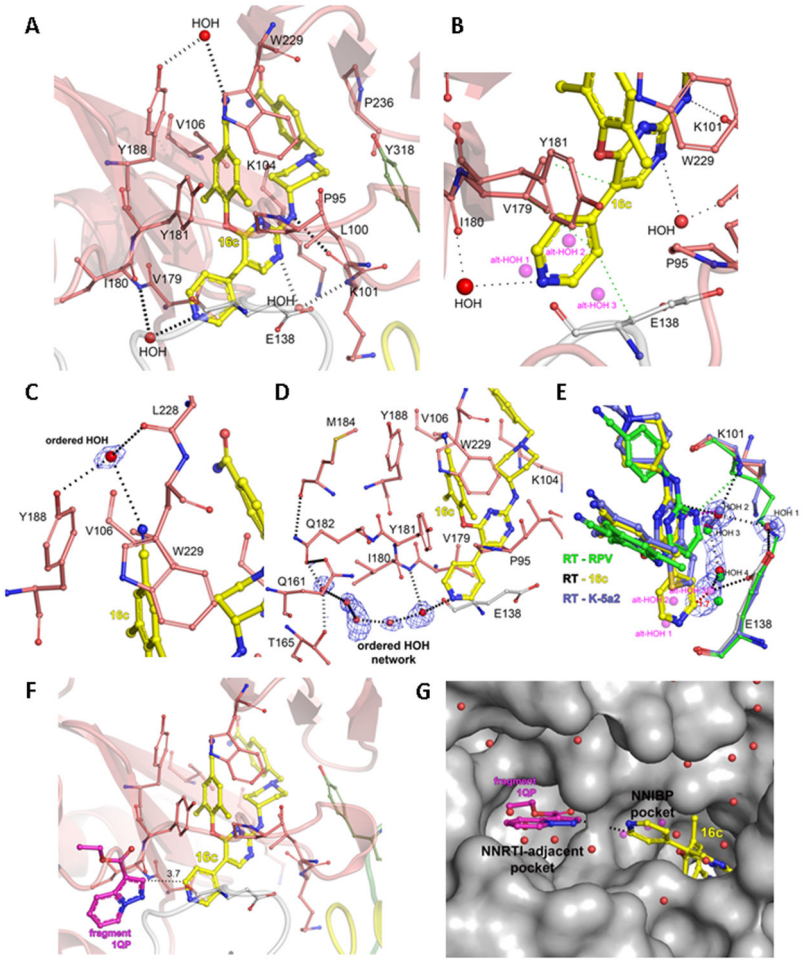

Figure 3.

Crystal structure of HIV-1 RT in complex with **16c** (PDB ID: 7KWU). (A) **16c** binding in the NNIBP, with hydrogen bonding-interactions with RT and water molecules. (B) Detail of the binding of the 4-pyridyl substituent. (C-E) Water molecule and networks involved in binding of **16c**. (F) Overlay of the RT-**16c** structure with RT-RPV-1QP fragment (bound to the NNRTI Adjacent site, PDB ID 4KFB), with the distance between nearer atoms of each. (G) Surface representation of (F), displaying the labeled pockets, with surrounding crystallographic water molecules from the RT-**16c** structure. Color legend for carbon atoms: (i) RT p66 subdomains: fingers in blue, palm in dark red, thumb in green, and connection in yellow; (ii) RT p51 subunit in white, and water molecules in red unless otherwise indicated.

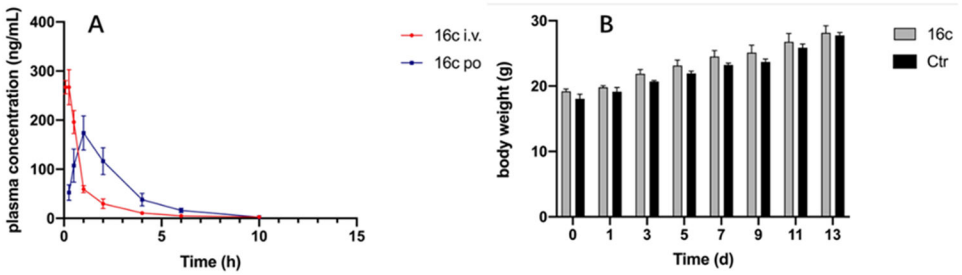

Figure 4.

(A) The plasma concentration–time profiles of **16c** in rats following oral administration (20 $mg.kg^{-1}$) and intravenous administration (2 $mg.kg^{-1}$). (B) The relative body weight changes of Kunming mice in different groups.

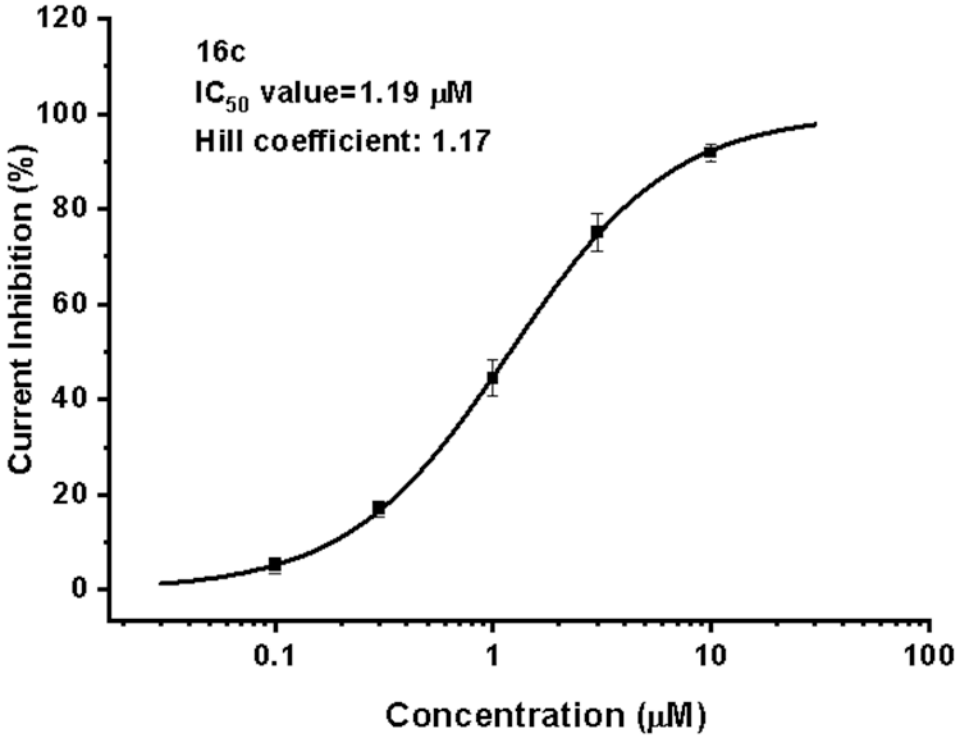

Figure 5.
Activity of **16c** against hERG potassium channel in HEK293 cells.

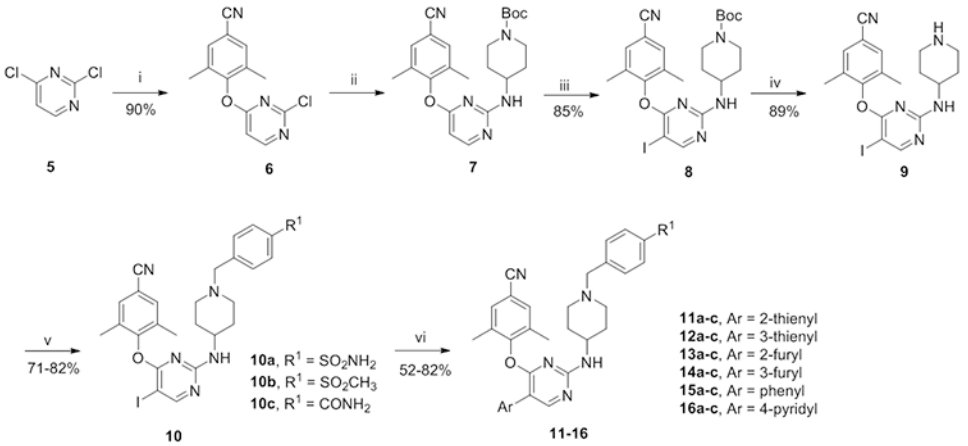

Scheme 1.

Synthesis of 11-13[a]

[a] **Reagents and conditions:** (i) K_2CO_3, DMF, 4-hydroxy-3,5-dimethylbenzonitrile, r.t.; (ii) K_2CO_3, DMF, *tert*-butyl 4-aminopiperidine-1-carboxylate, 120°C; (iii) NIS, HOAc, CH_3CN, r.t.; (iv) TFA, DCM, r.t.; (v) K_2CO_3, DMF, r.t.; (vi) $Pd(PPh_3)_4$, K_2CO_3, DMF, H_2O, 100°C.

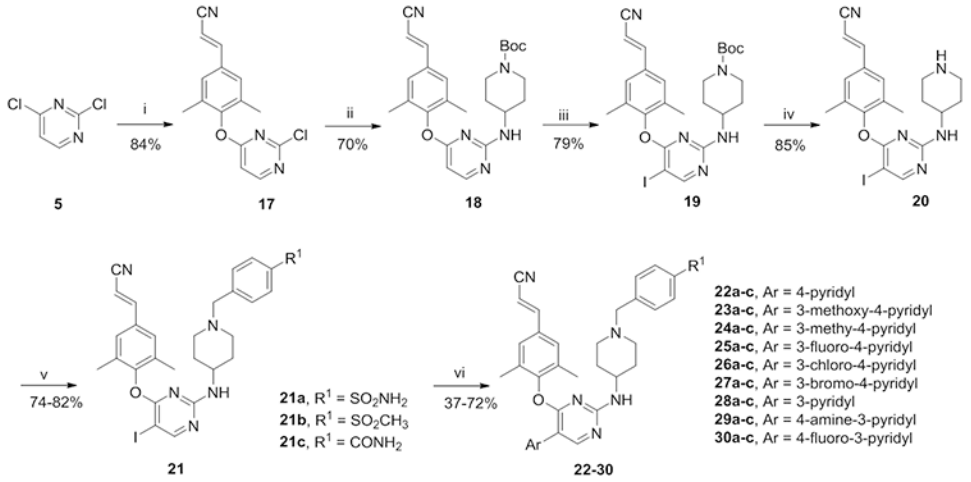

Scheme 2.

Synthesis of **22-30** [a]

[a] **Reagents and conditions:** (i) (*E*)-3-(4-hydroxy-3,5-dimethylphenyl)acrylonitrile, K_2CO_3, DMF, r.t.; (ii) K_2CO_3, DMF, *tert*-butyl 4-aminopiperidine-1-carboxylate, 120°C; (iii) NIS, HOAc, CH_3CN, r.t.; (iv) TFA, DCM, r.t.; (v) K_2CO_3, DMF, r.t.; (vi) $Pd(PPh_3)_4$, K_2CO_3, DMF, H_2O, 100°C.

Table 1.

Anti-HIV activity, cytotoxicity and SI values of target compounds **11-16**.

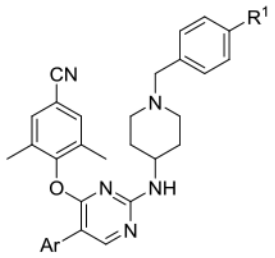

11-16

Compds	Ar	R[1]	EC_{50}(nM)[a]			CC_{50} (μM)[b]	SI[c]	
			IIIB	RES056	ROD		IIIB	RES056
11a		SO_2NH_2	4.57±0.50	103±33.8	≥33410	53.8±41.9	11787	520
11b		SO_2CH_3	4.01±0.73	134±29.8	>8383	8.38±4.50	2091	62
11c		$CONH_2$	3.34±1.17	115±6.71	>9263	9.26±3.75	2773	80
12a		SO_2NH_2	5.09±1.50	209±40.7	>6124	6.13±1.98	1205	29
12b		SO_2CH_3	4.92±1.60	253±83.8	>4252	4.25±1.45	863	17
12c		$CONH_2$	4.22±0.38	415±76.4	>37332	37.3±4.31	8838	90
13a		SO_2NH_2	4.40±1.26	218±100	>11187	11.2±2.92	2539	51
13b		SO_2CH_3	4.52±1.03	233±45.6	>7459	7.45±3.27	1650	32
13c		$CONH_2$	5.78±1.45	254±66.4	>7347	7.35±2.46	1271	29

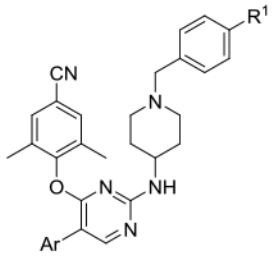

11-16

Compds	Ar	R[1]	EC$_{50}$(nM)[a]			CC$_{50}$ (μM)[b]	SI[c]	
			IIIB	RES056	ROD		IIIB	RES056
14a		SO_2NH_2	2.51±0.73	161±40.9	>29105	29.1±8.99	11611	180
14b		SO_2CH_3	4.75±0.94	172±9.51	>55821	55.8±13.7	11748	323
14c		$CONH_2$	3.40±0.48	108±24.5	>181990	181±7.10	53580	1685
15a		SO_2NH_2	5.14±2.08	427±62.6	>14067	14.1±4.72	2735	33
15b		SO_2CH_3	4.93±1.75	590±103	>12118	12.1±5.26	2456	21
15c		$CONH_2$	5.11±2.13	562±75.9	>13367	≥13.37	≥2618	≥24
16a		SO_2NH_2	2.59±0.46	111±35.9	>5669	5.67±0.27	2189	51
16b		SO_2CH_3	5.93±2.79	244±45.8	>17197	17.2±4.09	2897	70
16c		$CONH_2$	3.75±0.40	24.4±3.06	>35998	36.0±4.85	9603	1474
ETR	-	-	2.80±0.65	37.6±2.09	>4594	>4.59	>1638	>122
RPV			1.00±0.27	10.7±7.96	-	3.98	3989	371

[a] EC$_{50}$: concentration of compound required to achieve 50% protection of MT-4 cell cultures against HIV-1-induced cytopathicity, as determined by the MTT method.

[b] CC_{50}: concentration required to reduce the viability of mock-infected cell cultures by 50%, as determined by the MTT method.

[c] SI: selectivity index, the ratio of CC_{50}/EC_{50}.

Table 2.

Activity against mutant HIV-1 strains of target compounds **11-16**.

Compds	EC_{50}(nM)[a]					
	L100I	**K103N**	**Y181C**	**Y188L**	**E138K**	**F227L+V106A**
11a	5.92±1.11	5.39±1.58	10.7±3.63	9.31±1.28	7.71±1.86	30.2±2.43
11b	8.93±3.62	5.71±1.46	11.6±5.99	15.4±4.30	6.27±0.35	38.4±9.65
11c	14.7±2.59	5.15±0.90	10.2±4.68	17.9±5.48	8.85±1.90	75.4±21.9
12a	15.4±5.52	4.70±0.97	12.3±2.21	30.3±5.84	19.7±6.52	85.3±15.6
12b	20.3±5.08	4.75±1.16	11.7±2.04	27.2±9.63	10.6±2.80	67.5±21.4
12c	62.6±12.1	5.52±0.85	26.4±6.79	30.0±12.49	22.0±7.28	325±95.5
13a	20.9±10.5	5.33±1.42	24.8±11.8	36.5±14.3	24.5±5.57	128±46.6
13b	20.4±4.24	5.92±0.90	26.4±10.0	28.8±10.6	27.4±7.81	110±32.1
13c	38.2±11.3	3.73±0.48	14.9±3.89	23.3±2.89	11.9±2.12	161±26.7
14a	13.6±7.53	3.00±0.27	9.35±3.88	15.3±5.08	13.0±1.13	63.2±11.5
14b	14.8±3.99	4.39±0.66	14.4±4.40	24.2±3.50	15.3±4.23	41.5±6.88
14c	10.1±1.75	3.44±0.16	9.81±1.49	21.1±3.27	11.2±4.12	307±7.28
15a	53.2±6.18	7.74±0.82	26.2±7.23	33.2±2.51	24.5±2.10	219±62.4
15b	71.7±12.4	11.7±2.25	33.7±12.1	35.5±1.47	32.1±4.55	218±47.6
15c	151±84.2	9.15±2.14	28.7±6.81	30.5±8.73	17.1±5.43	393±28.4
16a	10.6±2.13	2.33±0.61	6.93±1.36	21.4±3.82	8.12±0.17	45.9±2.43
16b	17.4±9.08	4.40±0.96	10.8±2.43	18.5±3.37	9.19±0.79	79.4±13.9
16c	4.26±0.62	3.79±0.42	6.79±1.49	6.79±2.82	10.9±5.63	10.4±5.30
ETR	5.42±1.80	2.71±0.96	13.6±3.56	13.7±4.85	7.17±2.78	17.5±5.14
RPV	1.54±0.00	1.31±0.36	4.73±0.48	79.4±0.77	5.75±0.11	81.6±21.2

[a] EC_{50}: concentration of compound required to achieve 50% protection of MT-4 cell cultures against HIV-1-induced cytopathicity, as determined by the MTT method.

Table 3.

Anti-HIV activity, cytotoxicity and SI values of target compounds **22-30**.

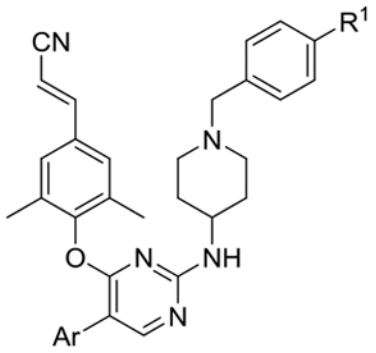

Compds	R_1	R_2	EC_{50}(nM)[a]		CC_{50} (μM)[b]	SI[c]	
			IIIB	RES056		IIIB	RES056
22a		SO_2NH_2	4.60±1.14	22.9±7.07	9.25±5.17	2011	404
22b		SO_2CH_3	5.74±1.38	26.3±6.99	7.20±5.41	1255	273
22c		$CONH_2$	4.19±0.45	23.3±7.67	10.2±6.69	2428	436
23a		SO_2NH_2	5.75±1.27	34.3±13.2	5.50±1.98	957	160
23b		SO_2CH_3	3.95±0.54	30.0±12.4	2.10±0.95	533	70
23c		$CONH_2$	7.28±1.27	40.3±10.7	6.27±1.21	861	156
24a		SO_2NH_2	4.16±0.98	23.0±5.85	4.37±1.15	1105	190
24b		SO_2CH_3	4.55±0.61	31.5±5.50	5.34±2.87	1174	169
24c		$CONH_2$	3.53±0.38	18.1±0.30	6.51±2.82	1845	358

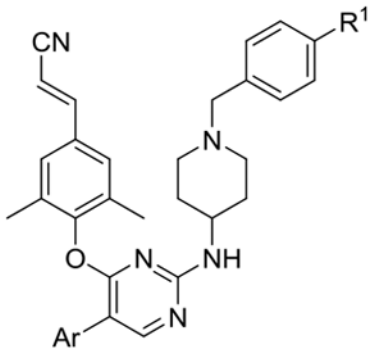

Compds	R_1	R_2	EC_{50}(nM)[a]		CC_{50} (μM)[b]	SI[c]	
			IIIB	RES056		IIIB	RES056
25a		SO_2NH_2	6.37±1.27	38.8±12.6	8.46±2.08	1326	218
25b		SO_2CH_3	4.75±1.19	25.1±7.23	5.03±1.72	1057	200
25c		$CONH_2$	8.26±1.79	53.4±30.9	15.5±5.32	1878	290
26a		SO_2NH_2	4.30±0.54	20.9±4.14	3.89±1.01	904	185
26b		SO_2CH_3	4.23±1.06	33.3±7.24	2.04±0.88	482	61
26c		$CONH_2$	4.14±0.43	81.7±61.7	19.1±1.66	4627	243
27a		SO_2NH_2	4.42±0.52	26.9±12.1	6.60±2.69	1493	246
27b		SO_2CH_3	4.52±0.55	33.2±9.31	3.21±0.61	711	97
27c		$CONH_2$	7.00±4.69	32.2±8.02	9.45±4.34	1351	293

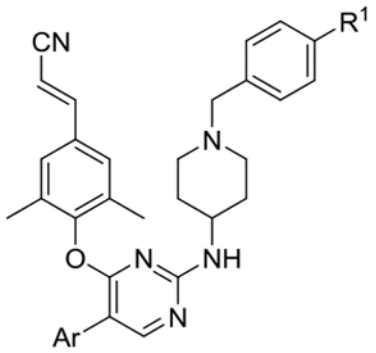

Compds	R_1	R_2	EC_{50}(nM)[a]		CC_{50} (μM)[b]	SI[c]	
			IIIB	RES056		IIIB	RES056
28a		SO_2NH_2	5.04±2.07	25.8±9.45	20.4±4.11	4063	793
28b		SO_2CH_3	4.57±1.24	22.4±1.87	23.5±0.96	5151	1049
28c		$CONH_2$	4.78±2.57	23.1±3.80	25.3±1.84	5297	1092
29a	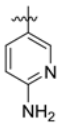	SO_2NH_2	5.80±1.37	33.5±6.89	2.91±0.65	503	87
29b	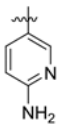	SO_2CH_3	5.29±2.14	26.2±4.80	2.36±0.93	447	90
29c	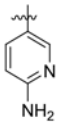	$CONH_2$	6.56±2.11	30.2±6.55	12.8±3.73	1956	424
30a	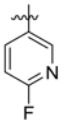	SO_2NH_2	5.80±1.53	28.2±6.82	17.1±4.82	2956	607
30b	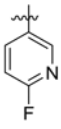	SO_2CH_3	6.04±1.76	25.5±2.89	6.05±1.18	1003	237

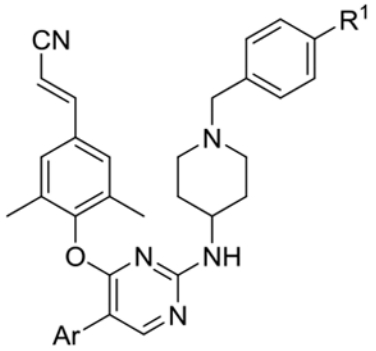

Compds	R_1	R_2	EC_{50}(nM)[a]		CC_{50} (μM)[b]	SI[c]	
			IIIB	RES056		IIIB	RES056
30c	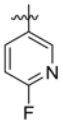	$CONH_2$	4.56±1.49	20.4±0.98	20.9±3.65	4586	1021
ETR	-	-	3.53±0.70	52.2±24.2	>4.59	>1300	>88
RPV			1.0±0.27	10.7±7.96	3.98	3989	371

[a] EC_{50}: concentration of compound required to achieve 50% protection of MT-4 cell cultures against HIV-1-induced cytopathicity, as determined by the MTT method.

[b] CC_{50}: concentration required to reduce the viability of mock-infected cell cultures by 50%, as determined by the MTT method.

[c] SI: selectivity index, the ratio of CC_{50}/EC_{50}.

Table 4.

Activity against mutant HIV-1 strains.

Compds	EC_{50}(nM)[a]					
	L100I	**K103N**	**Y181C**	**Y188L**	**E138K**	**F227L+V106A**
22a	5.87±1.99	4.91±1.47	24.2±8.96	27.1±9.19	11.1±2.21	23.7±13.8
22c	5.62±1.98	3.84±0.66	7.14±1.07	23.0±4.49	8.66±0.37	35.5±21.6
28a	7.85±3.59	6.25±4.17	9.95±0.96	25.1±12.7	11.9±2.35	12.2±2.27
28b	10.7±1.54	5.42±2.35	10.3±1.32	22.7±9.14	12.2±4.53	13.2±3.41
28c	10.8±1.66	5.76±2.33	10.1±1.62	25.5±12.3	11.3±2.74	21.7±9.43
29c	11.3±3.73	6.66±0.50	12.0±1.45	54.2±10.9	15.4±3.98	15.4±3.22
30a	11.4±2.85	7.50±1.61	15.4±2.24	36.7±6.86	49.1±31.5	23.1±13.9
30c	5.76±3.50	5.97±1.49	10.3±0.53	30.1±10.9	11.7±6.16	27.5±10.5
ETR	11.7±7.44	3.77±1.06	16.6±5.36	15.4±4.72	18.8±8.52	26.9±2.30
RPV	1.54±0.00	1.31±0.36	4.73±0.48	79.4±0.77	5.75±0.11	81.6±21.2

[a] EC_{50}: concentration of compound required to achieve 50% protection of MT-4 cell cultures against HIV-1-induced cytopathicity, as determined by the MTT method.

Author Manuscript

Author Manuscript

Author Manuscript

Table 5.

Inhibitory activity against WT HIV-1 RT

Compds	IC_{50} (μM)[a]	Compds	IC_{50} (μM)[a]
14a	0.092±0.002	**22a**	0.143±0.003
16c	0.113±0.032	**22c**	0.102±0.013
NVP	0.510±0.140	**ETR** [b]	0.011±0.000

[a] IC_{50}: inhibitory concentration required to inhibit biotin deoxyuridine triphosphate (biotin-dUTP) incorporation into WT HIV-1 RT by 50%.

[b] Results from reference 11.

Table 6.

Pharmacokinetic profile of **16c**[a]

Subject	$T_{1/2}$ (h)	T_{max} (h)	C_{max} (ng/mL)	AUC_{0-t} (h*ng/mL)	$AUC_{0-\infty}$ (h*ng/mL)	CL (mL/min/kg)	F (%)
16c (iv)[b]	2.46±0.56	0.033	278±31.2	293±32.7	303±31.1	110±10.9	-
16c (po)[c]	1.74±0.65	1.00±0.00	174±12.5	460±296	466±294	-	15.3

[a] PK parameter (mean ± SD, n = 3)

[b] Dosed intravenously at 2 mg/kg

[c] Dosed orally at 20 mg/kg.